Department of AERONAUTICS and ASTRONAUTICS
STANFORD UNIVERSITY

AN INTRODUCTION TO INSTABILITY

(A Pictorial Survey of the Stability of Bars, Plates, and Shell Bodies)

by

Wilfred H. Horton, Stanley C. Bailey, and Beatrice H. McQuilkin

This paper is a summary of and an extension to the film
Buckling Phenomena
presented at the ASTM Annual Meeting
in
Atlantic City, N. J.
in
June 1966

The work here presented was supported by the
United States Army Aviation Materiel Laboratories Under
Contracts DA 44-177-AMC-115(T) and DA 44-177-AMC-258(T)
and the
Air Force Office of Scientific Research Under Contract AF 49(638) 1495

AN INTRODUCTION TO INSTABILITY

(A Pictorial Survey of the Stability of Bars, Plates, and Shell Bodies)

by

Wilfred H. Horton, Stanley C. Bailey, and Beatrice H. McQuilkin

This paper is a summary of and an extension to the film

Buckling Phenomena

presented at the ASTM Annual Meeting

in

Atlantic City, N. J.

in

June 1966

The work here presented was supported by the

United States Army Aviation Materiel Laboratories Under

Contracts DA 44-177-AMC-115(T) and DA 44-177-AMC-258(T)

and the

Air Force Office of Scientific Research Under Contract AF 49(638) 1495

A well-designed structure must possess sufficient strength to sustain a given system of applied forces without rupturing or crushing of the material and at the same time it must be sufficiently stable to resist these forces without excessive alteration in the geometric form in which it has been designed. It is this latter problem with which this paper is concerned. The purpose is to present a visual representation of the instability modes for a wide range of practical bodies. However, the paper presents not only illustrations of the deformed shapes but also outlines some pertinent aspects of our knowledge, both theoretical and experimental of these behavior patterns.

The first studies in the field of elastic stability were made by Leonard Euler in 1744. The problem with which he was concerned was the behavior of a column under direct load. The analysis which he made was concerned with a long column and the result he derived still applies to this case. This classic computation shows that the critical load for a long column, with pinned ends, in which the axial force is constrained to always act in the direction of the column before buckling is given by

$$P_{cr} = \frac{\pi^2 EI}{L^2}$$

where E = the elastic modulus of the column material
I = the second moment of the cross sectional area
L = the length of column between pin centers

It is important to remark in connection with this problem that when the conditions at the end, or the constraint on the force, or both are changed the critical load is altered.

For various combinations of load, load direction and end conditions corresponding critical loads are given in Table 1.

In all cases it is apparent that the load carrying capability is not influenced by the specific strength of the material. The modulus is the only material property of significance. Thus, a long column of high tensile steel has the same buckling load as a long column of low tensile steel.

In reality columns are not always long, perfect in form or end condition, indeed, the true situation is the antithesis of this. Thus, the practical engineer becomes confronted with significant variations from the conditions of applicability

Table 1--Critical Load for a Column With Various End Conditions and Load Application Through a Fixed Point

$$P_{cr} = \frac{C \pi^2 EI}{L^2}$$

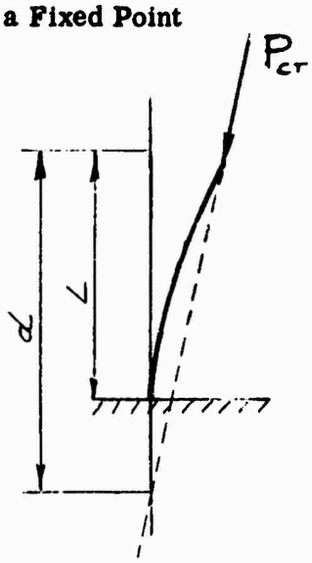

End Condition	Fixed Point Ratio (d/L)	Restraint Coefficient C
One End Built-In Other End Free	∞	0.25
	10	0.272
	5	0.298
	2	0.417
	1.5	0.531
	1	1
	0.6	1.76
	0.4	1.91
	0.2	2.00
One End Built-In Other End Pinned	0	2.05
Both Ends Built-In	0	4.00

of Euler's theory in all respects. Geometric variations about the mean, eccentricity of load, and stresses outside the confines of Hooke's law. Despite significant contributions to the theory during the 19th century it was not until von Kármán rationalized the situation by a logical extension of the Euler theory that a satisfactory theory of Euler buckling existed. According to this study the average experimental value of critical buckling stress is about 98 per cent of the theoretical load level.

The Karman-Engesser law is very slightly different to that of Euler. It is in fact

$$P_{cr} = C.\frac{\pi^2 E_r I}{L^2}$$

where C = the restraint coefficient

and E_r = the so-called reduced modulus which lies between E_t (the tangent modulus) and E (Young's modulus) and depends upon the cross section shape.

For all practical purposes, however, it will usually suffice to make the computation on the basis that

$$P_{cr} = C.\frac{\pi^2 E_t I}{L^2}$$

As remarked earlier, it is impossible to obtain a strut which is perfect in form or to load it without obtaining an eccentricity.

Thus, even today, empiricism plays an important part in the prediction of column behavior and the literature contains many references to empirical and semiempirical laws for column behavior. Two of the most common of these are Rankin's formula and the Johnson parabolic formula.

The variations from ideal form mean, of course, that a strut will bow immediately upon loading and the Euler stress is therefore not sharply defined, although as it is approached the deflection increases with great rapidity. R. V. Southwell has demonstrated that the equation

$$P_E \cdot \frac{\delta}{P} - \delta = \text{constant}$$

is a sufficiently accurate description of the load displacement relationship.

In this formula

P_E = Euler load

P = actual load

S = a deflection (for sensitivity measured at point of maximum displacement).

Hence, by plotting δ against $\frac{\delta}{P}$ one obtains a straight line, the slope of which is P_E and the intercept with the appropriate axis is the initial eccentricity.

The maximum stress σ_{max} produced in a ball-ended strut loaded at both ends with the same eccentricity e, measured from a principal axis, XX, is given by the well-known secant formula

$$\sigma_{max} = \sigma \left\{ 1 + \frac{e\, y_{max}}{r^2} \sec \left[\frac{L}{2r} \left(\frac{\sigma}{E_t} \right)^{1/2} \right] \right.$$

where σ = average stress

E_t = tangent modulus

y_{max} = distance of extreme fiber from XX axis

and r = the appropriate radius of gyration

The type of overall failure, termed Euler column failure, depicted in Figs. 1 and 2 is, of course, not the only kind of failure which can be experienced with columns, particularly when their cross sections are of open form.

The photographs of Figs. 3(a-c) illustrate a different mode of instability for open section struts. The type of instability herein demonstrated is termed local instability. In members with flat sides, local instability is defined as that mode of distortion in which the meets of adjacent sides remain stationary. Thus, the sides buckle, as plates elastically supported along their edges, with a half wavelength approximately equal to the distance apart of the free edges. This type of instability is very clearly shown in the pictures already referenced.

In general, buckling is not restricted to the free flanges, the web of the section can likewise buckle. This is clearly seen in Figs. 4(a,b).

Analysis is in fair agreement with observed behavior for Z, U and I sections. In practice, engineers tend to stabilize the free flanges by the addition of narrow lip flanges whose width is restricted to some five to ten times the thickness of the material.

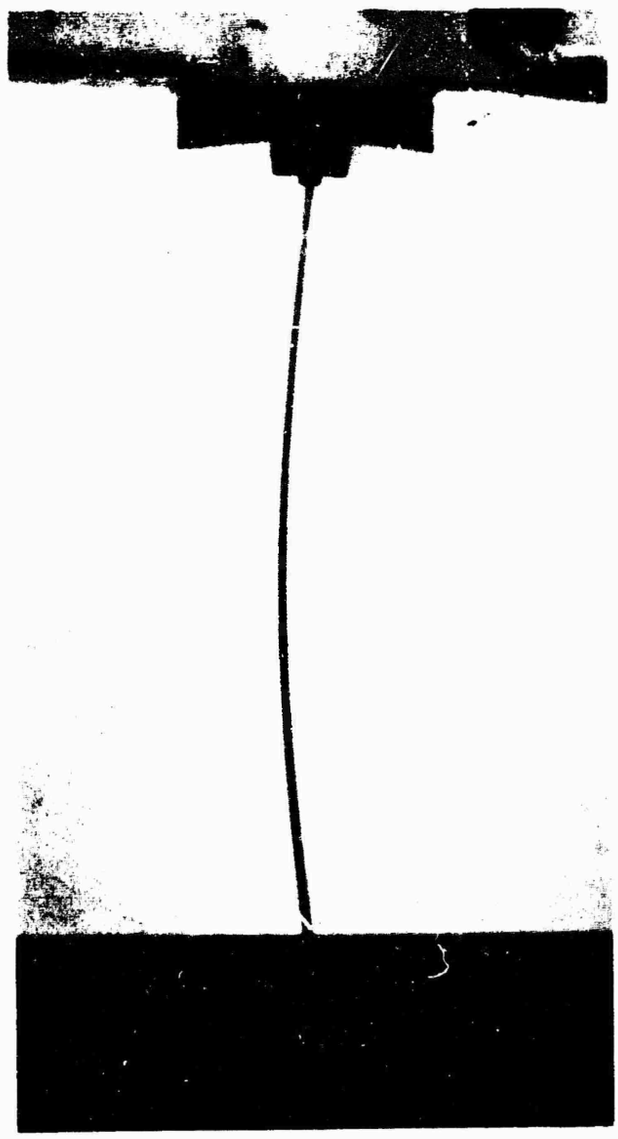

Fig. 1--Typical Euler Buckling of a Long Column With Both Ends Pinned.

Fig. 2--Typical Euler Buckling of a Long Column With Both Ends Built-In.

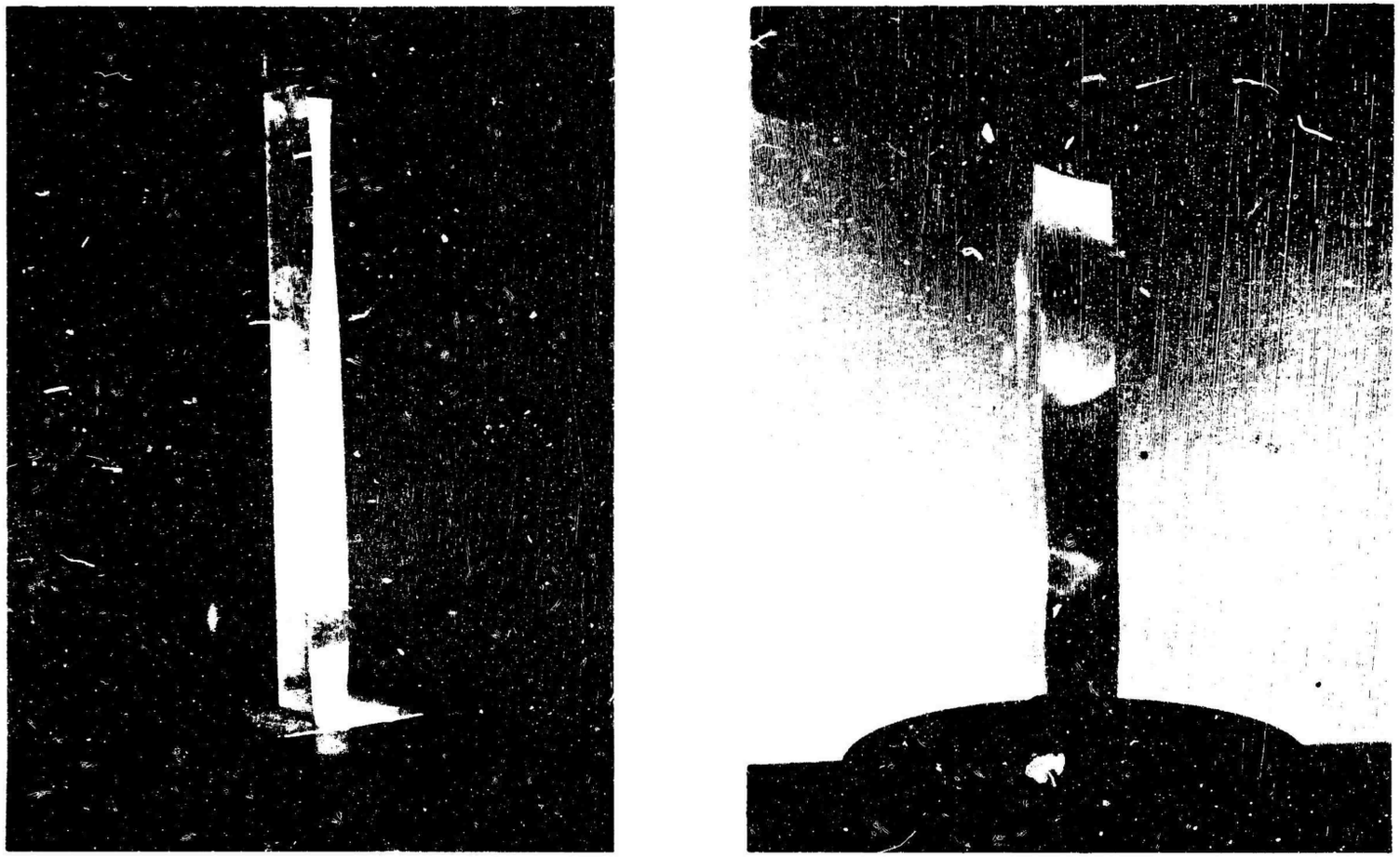

Fig. 3(a)--Local Buckling of L-Shaped Struts.

Fig. 3--Local Instability of Thin-Walled Open Section Struts.

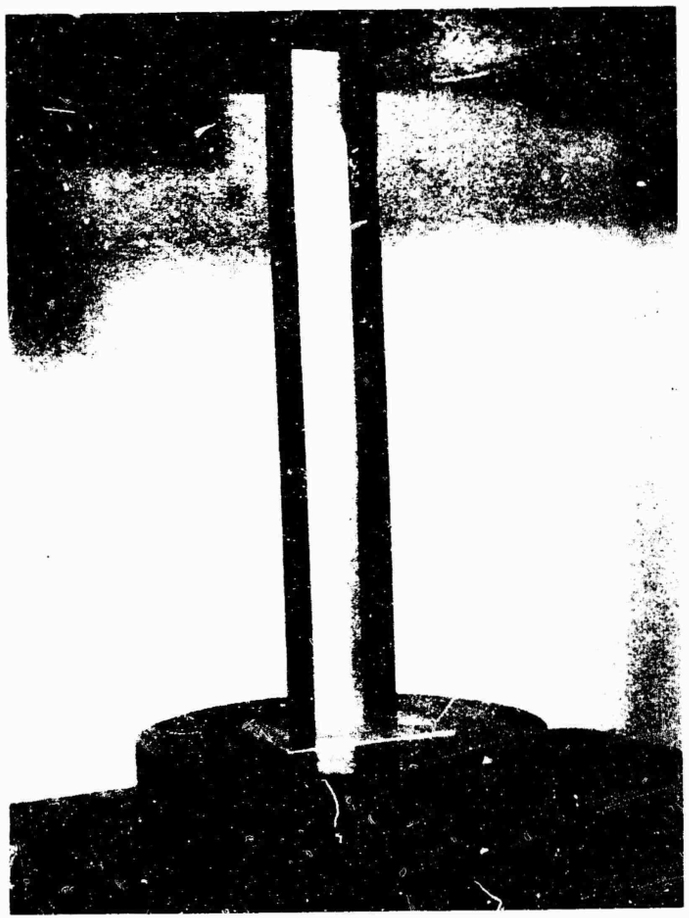

Fig. 3(b)--U-Shaped Strut Loaded Below Critical Load.

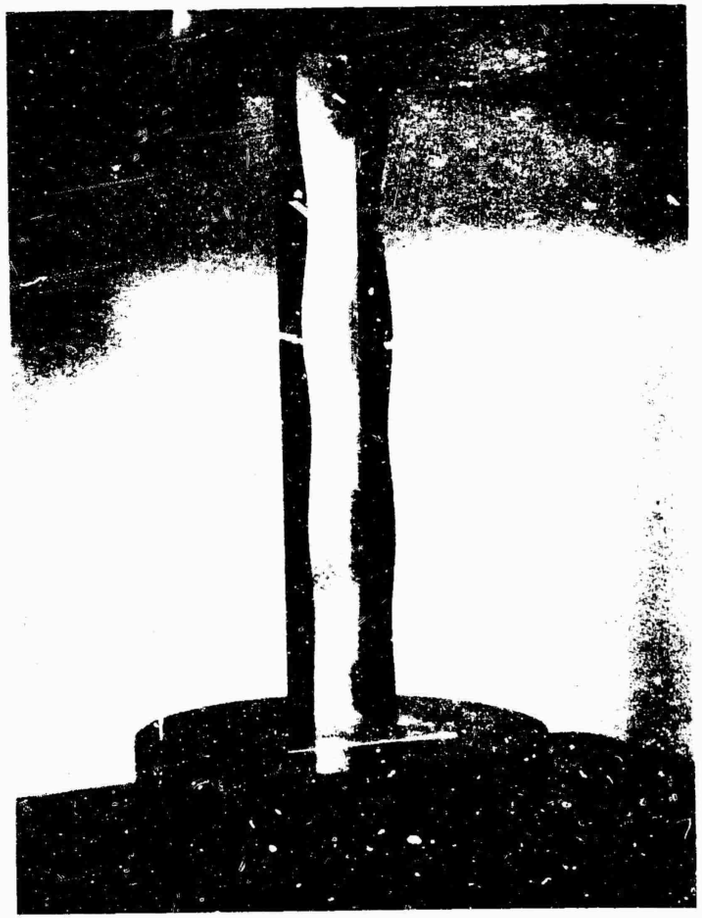

Fig. 3(c)--Local Buckling of U-Shaped Strut.

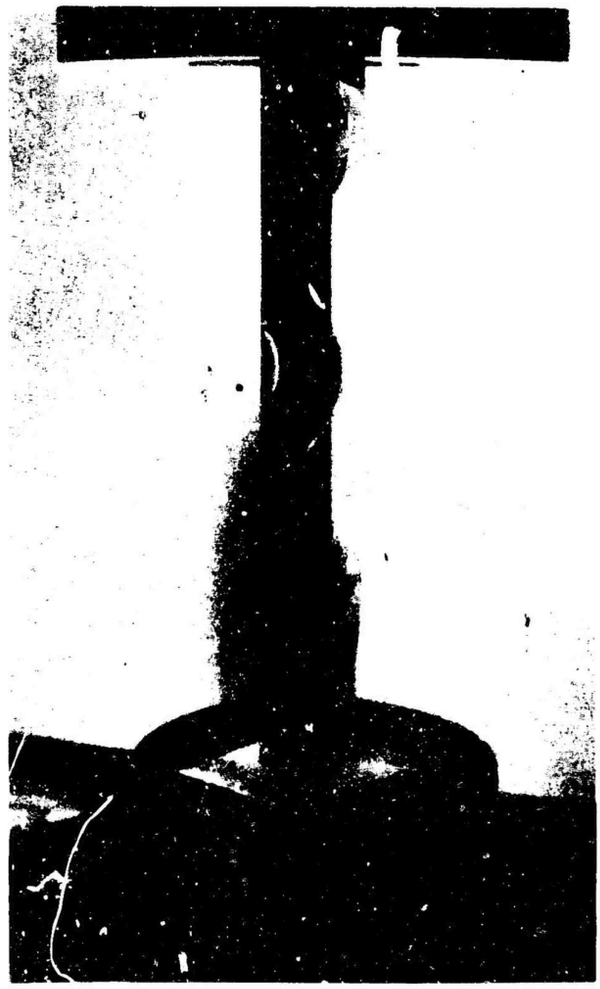

Fig. 4(a)--U-Shaped Strut.

Fig. 4--Local Instability of Thin-Walled Open Section Struts With Buckled Web Section.

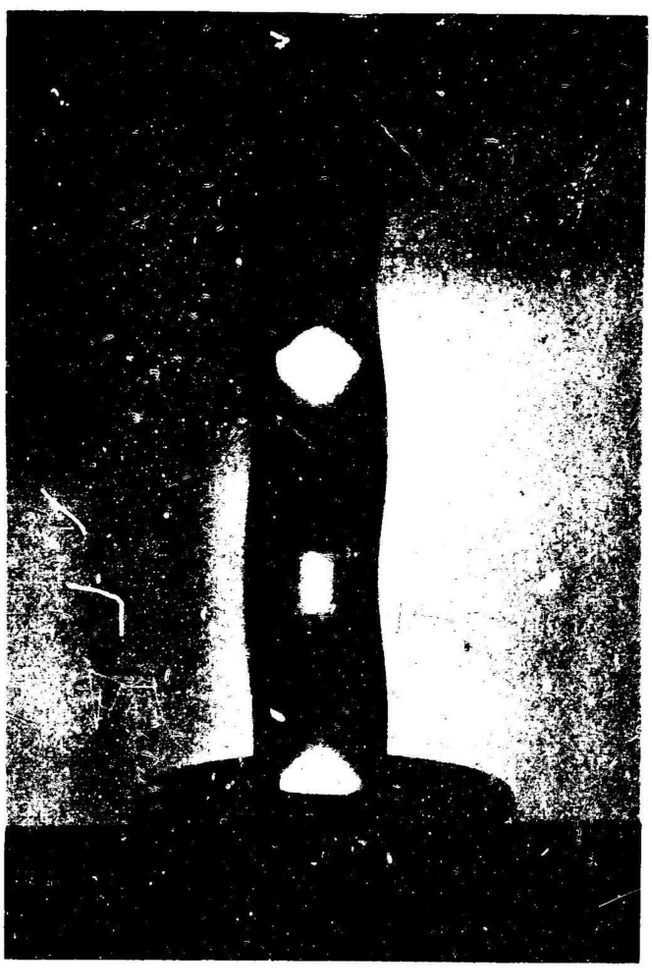

Fig. 4(b)--Z-Shaped Strut.

Buckling of this kind does not imply failure. Columns will continue to carry load after they are unstable but, of course, they lose stiffness.

In all cases the critical stress can be expressed by an equation of the type

$$\sigma_{cr} = KE\left(\frac{t}{h}\right)$$

where K = the local buckling stress coefficient
t = the thickness of the 'sheet'
h = the length dimension

As the stress on any column member rises, the cross section experiences distortions which may be local or extend over the length of the member, as we have already shown. Such distortion of the section causes a shearing stress to develop; a shearing which is proportional to the magnitude of the applied end load and the slope of the deflective region. This shearing produces forces on open sections which may well cause rotation; particularly, if the torsional stiffness to the section is low, as it will be when the element is thin-walled. The section shown in the test machine in Fig. 5 is an L shaped section, in which the leg is wide in relation to its thickness, and in relation to the length of the member. We see (Fig. 5) that it does not bow, but rotates. A torsional failing mode was induced as a consequence of the reaction to the axial compressive force. Nearly all open sections may be subject to this mode of instability. Very little specific information is available and few experimental checks of the theory have been made.

In general, a thin-walled open section strut, under a central load, will buckle in a mode involving flexure about the principal axis and twist about the flexural axis. However, if the shear center coincides with the centroid, the mode involving only twist about the flexural axis occurs. This is the pure torsional instability mode. The coincidence of the two points is possible only in sections with double or point symmetry. In unsymmetrical sections, it is often found that a combined flexure cum-torsion mode gives considerably lower failing stress than either of those corresponding to the pure component modes The test sequence shown demonstrates this point, Figs. 5,6. The second specimen, the longer L, buckles in a torsion flexure mode. When the length of side is reduced to a half, the mode becomes more predominantly the Euler column type, as in Fig. 6(c). The critical load for the two shapes are identical. The

Fig. 5--Pure Torsional Failing Mode of Thin-Walled L-Shaped Strut.

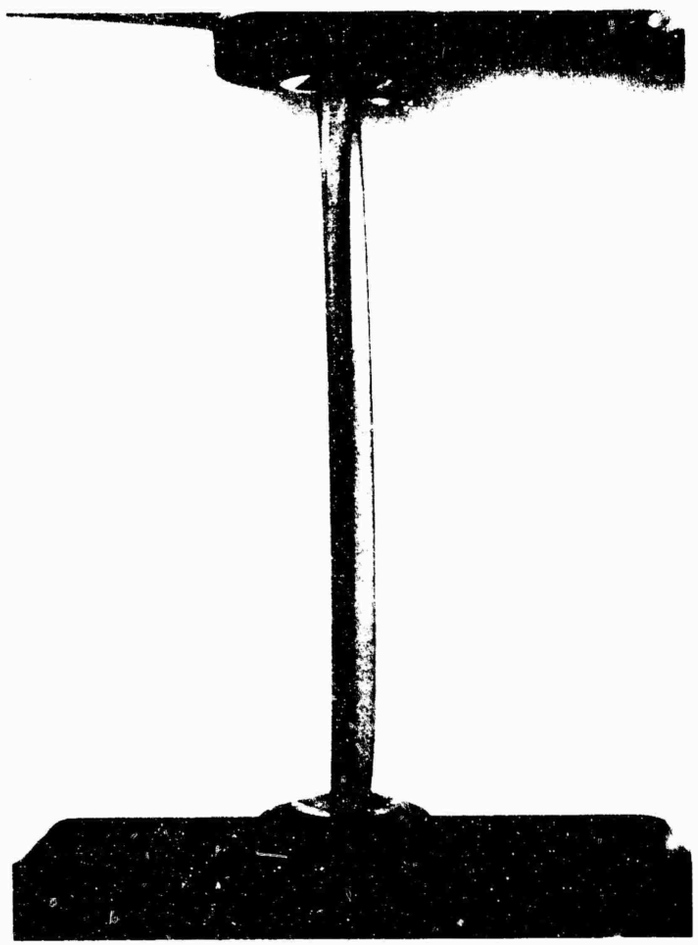

Fig. 6(a)--Predominate Torsional Failure.

Fig. 6(b)--Combined Flexure Cum-Torsional Mode.

Fig. 6--Change in Buckling Mode of an L-Shaped Strut by Alteration of Cross Section Geometry.

Fig. 6(c)--Predominate Euler Failure Caused by Reducing the Width of Flanges.

efficiencies are in the ratio of two to one. If we reduced the column length then we could arrive at the situation in which the reduced cross section would have much higher load carrying capability than its larger counterpart. Just as in the case of pure flexure, the critical load to produce instability, is severely dependent upon the nature of any end constraint to which the member is subjected. Boundary conditions always play an important role in instability problems. The pure torsional instability mode can be associated with a stress σ_T such that

$$\sigma_T = \frac{GJ + C \cdot \frac{\pi^2}{L^2} E\Gamma}{I_p}$$

where G = the shear modulus

E = Young's modulus

I_P = the polar moment of inertia with reference to an axis through the shear center

Γ = the total warping constant

J = the torsion constant for the section

As with other problems of struts the constant, C, depends upon the conditions of end fixity -- for the case when the ends are restrained against twist but are free to warp $C = 1$, when completely built-in $C = 4$.

For arbitrary cross sections the buckling stress σ may be found from the largest root in the following cubic in $\frac{1}{\sigma}$.

$$\left(1 - \frac{\sigma_x}{\sigma}\right)\left(1 - \frac{\delta_y}{\sigma}\right)\left(1 - \frac{\delta_T}{\sigma}\right) - \left(1 - \frac{\delta_x}{\sigma}\right)\left(\frac{X}{r_p}\right)^2 - \left(1 - \frac{\sigma_y}{\sigma}\right)\left(\frac{Y}{r_p}\right)^2 = 0.$$

In this equation

σ_x, σ_y = the Euler stresses for flexure about principal axes

X, Y = the coordinates of the shear center with respect to the principal axes

r_p = the polar radius of gyration with respect to the axis through the shear center

The conditions of applicability of the equation are that the values of σ_x, σ_y and σ_T must correspond to the appropriate boundary conditions. For the case when the member is torsion restrained but free to warp σ_x, σ_y are the values for a ball ended strut and σ_T has a constant C = 1.0. In the built-in case C becomes 4 and the Euler values are likewise those for the encastré strut.

The initial buckling of flat plates in compression is a subject which has received considerable attention both from experimental and theoretical viewpoints. The classic literature contains many references to such behavior. It is seen from Fig. 7 that such plates buckle in waveforms which are essentially sinusoidal.

The critical buckling stress is given by

$$\sigma_b = KE\left(\frac{t}{b}\right)^2$$

Where K is the buckling stress coefficient whose value depends upon the plate dimensions, the boundary conditions and the Poisson ratio for the material

t = the plate thickness

b = the plate dimension normal to load direction

E = Young's modulus of the material

Flat plates, like plate columns, will continue to carry load after buckling has occurred. The maximum strength under these conditions is a subject of interest. Analytical studies show that load values under these conditions are predictable with high accuracy.

The various modes of buckling associated with column members, flexural, local, torsional and flexural torsional instability have been demonstrated and discussed. Plate buckling in compression has also been considered. In modern aircraft, however, we are rarely concerned with simple struts and plates. Generally, structures are much more complex, semimonocoques. Semimonocoque or stressed skin structures, are those which rely upon the covering to resist and transmit shearing forces and part of the longitudinal forces. These structures are composed of the skin, or external covering together with longitudinal and transverse members; termed stringers and ribs, or frames, respectively. There are two design criterion to be chosen from.

Fig. 7--Sinusoidal Buckling of a Flat Plate Subjected to Uniform Axial Compression.

Under certain circumstances it may be desirable that there will be no wrinkling or buckling, particularly of the surfaces, before a given load is carried by the structure. In other cases, total failure is the important question. Four categories of instability are normally recognized. Buckling of the stringers between adjacent frames in a manner analogous to column behavior; local instability in a manner similar to that already depicted: general instability -- a type of buckling in which several stringers, several frames, and the covering, are simultaneously involved; buckling of the skins alone. Such buckling may be due to shear or, of course, it may be wrinkling. The instability mode known as wrinkling, is that in which the plate buckles as a strut elastically supported by the stringers.

Realistic structures for aeronautical application are, of course, never flat sided. Thus, in addition to the complexities which arise from the assemblage of plates, frames, and stringers there are additional difficulties due to curvature. The literature contains guides to the analysis of structures fabricated as defined but caution must always be exercised in their application. One most important difficulty occurs in a cylinder subjected to bending, e.g., a fuselage. The stringers may fail by an inward motion or by an outward motion. The particular mode is dependent upon the curvature, and the stress levels are widely different. The variation is due to the fact that in the one case there is an elastic foundation to be considered in the other there is not.

It must be pointed out, too, that the critical stresses for shells with stiffeners on the inside are different to those for shells with the same stiffeners on the outside.

These subjects are very complex and a detailed treatment is not feasible here.

Semimonocoque structures are rarely monolithic. Today's advanced technologies of machine tool control and metal-to-metal bonding have certainly made structures of a nearly monolithic type possible. Nevertheless, we still tend to fasten the many components together by rivets or spot welds. Plate buckling between such attachment points is termed interrivet buckling and is shown in Fig. 8 for a flat plate under axial compression.

The critical stress in such regions is normally computed from a column type formula in which the end fixity coefficient is given a value of 3.0. This seems fairly representative of the situation when snap head rivets are used.

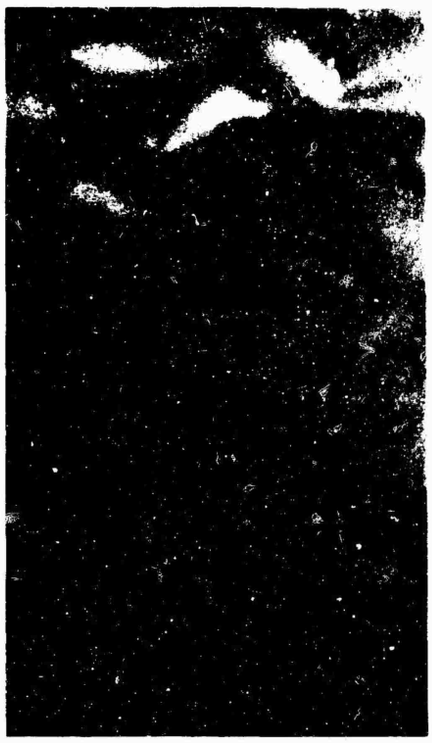

Fig. 8--Interrivet Buckling of a Flat Sheet Stringer Panel Loaded in Axial Compression.

Thus, $$\sigma_i = \frac{3\pi^2 E_t t^2}{12L^2}$$

Where E_t = tangent modulus at stress level σ_i

L = rivet pitch

t = plate thickness

It is important in the application of this formula to realize that local instability of the members to which the skin is attached must not occur at half wavelength comparable to the rivet pitch and that the plate may already be buckled at stress lower than σ_i.

The buckling of the strut between stringers has a detrimental effect on panel strength. First, it reduces the effective width of the sheet. Second, it reduces the support provided for the frames or stiffeners. This can often induce local stiffener failure. When this type of instability occurs, failure usually follows closely after the initial buckle.

Plate structures are subject to instabilities not only under compressive loads but also under shearing actions. The buckling stress under shear is given by an equation of the type

$$\tau_b = KE(t/b)^2$$

in which the value of K is dependent upon the panel dimensions and the conditions of edge support. t is the thickness of the plate and b its minor dimension. Curvature increases the critical stress levels and the formula developed for such cases is not substantially different to that given above but the value K now becomes dependent upon the ratio of b^2/Rt, where R is the radius of curvature, as well as the other parameters.

One important case of instability under shearing forces is found in the webs of beams. The beam shown in Figs. 9c-d is representative of this class of problem. The beam has two substantial flanges and a thin web with stiffeners. It is typical of many used in the horizontal and vertical stabilizers of aircraft. In the analysis of such beams the designer is faced with several problems which,

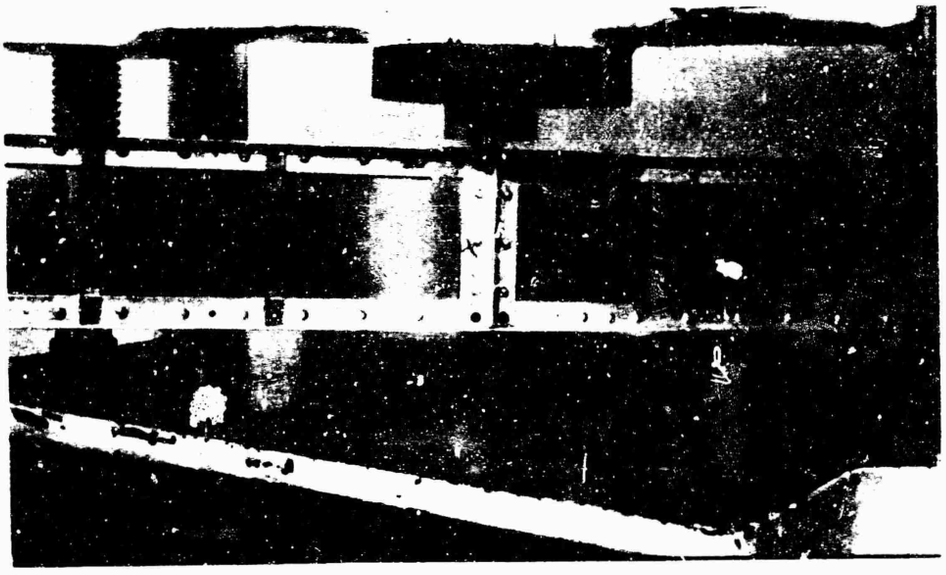

Fig. 9(a)--Beam Before Web Buckling.

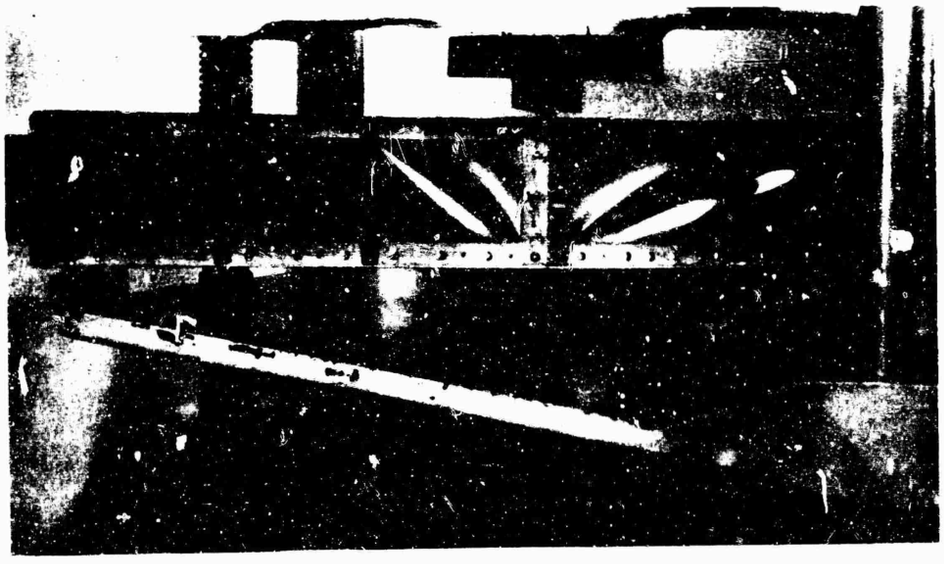

Fig. 9(b)--Beam After Web Buckling.

Fig. 9--Development of Diagonal Tension Field in a Thin-Web Beam.

Fig. 9(c)--Close-Up View of Web Buckle Without Stiffeners.

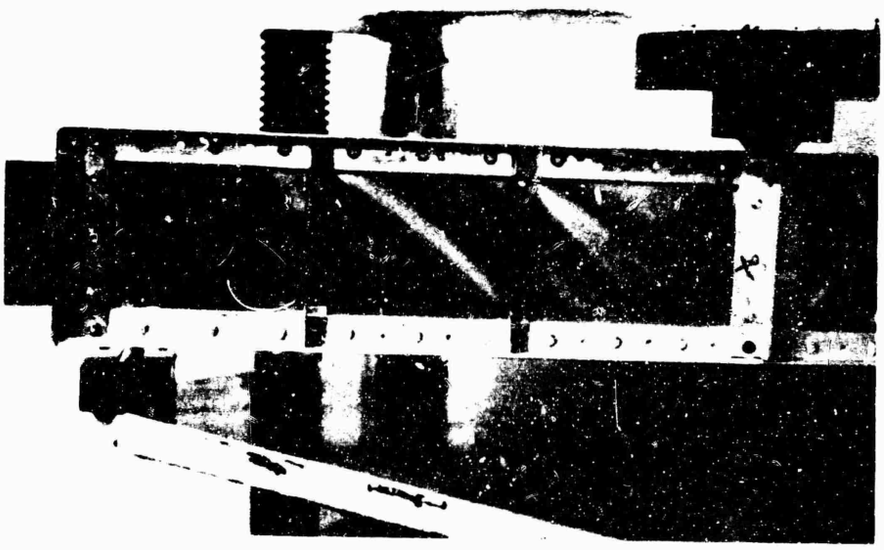

Fig. 9(d)--Close-Up View of Web Buckles Broken Up by Web Stiffeners.

until recently at any rate, were not present in civil engineering structural design. In general applications, shear webs are made so thick that buckling will not take place before the design load is reached. Buckling is then considered failure. Since initial buckling is certainly not the sign of imminent collapse, aircraft engineers must, in the interest of efficiency, raise the question of how much beyond this point can they go with certainty. They are concerned with a very thin web. An element at the center can, for the purposes of the argument, be chosen with sides of 45 degrees to the direction of shear. This element will be loaded then by equal normal stresses on its faces. Two will be compressive and two tensile. It is this compressive force which causes the plate to buckle -- to buckle in deep folds which are normal to the force. The shearing force is reacted by the tensile stresses which tend to fold the flanges together and to compress the stiffeners. This is the so-called tension field beam or Wagner beam. If the stiffening posts were not attached to the webs, then their load would be the vertical component of the tension field load corrected proportion between the stiffeners present. In practice they are usually attached, and these simple considerations no longer apply. To the tension field must be added the load which results from the fact that the stiffeners, where attached to the web, break up the web buckles which would otherwise be continuous along the beam web. These sheet waves deform the stiffeners torsionally and in bending tend to precipitate early failure due to localized stress conditions. The presence of flanged holes, not an infrequent occurrence, considerably complicates the question.

The simplest case -- the limiting case of a web with no compressive strength was treated first by Wagner. Under these conditions the following formula can be developed:

$$\sigma_t = \frac{2V}{ht} \cdot \frac{1}{\sin 2\alpha}$$

$$F_t = \frac{Vx}{h} - \frac{V}{2} \cot \alpha$$

$$F_c = -\frac{Vx}{h} - \frac{V}{2} \cot \alpha$$

$$F_v = -\frac{Vd}{h} \tan \alpha$$

where

V = applied shear load

h = effective web height

t = web thickness

d = vertical stiffener spacing

α = angle of buckles (45^{o})

σ_t = diagonal tension stress

F_t = axial force in the tension flange

F_c = axial force in the compression flange

F_v = axial force in the vertical stiffeners

x = distance from applied shear load

These simple equations are based upon the assumption that the flanges are infinitely stiff in bending but carry no shear load. Moreover, they are considered to be pinned to the verticals and pin connected at the fixed end of the beam. Where the highest efficiency is needed these assumptions are too conservative. More refined analysis is to be found in the literature. Generally speaking, the web stiffeners are so stiff that the web sheet will buckle between them without causing their failure. However, it is always wise to check that the stabilizing posts have sufficient stiffness to ensure this. Analytical solutions to this question have been made and are reasonably reliable.

A problem, which is met in structural engineering but rarely in aeronautical, is that of lateral instability of beams.

Beams without lateral support in which the bending rigidity in the plane of bending is large compared to the lateral bending rigidity will buckle in this mode when the load reaches a critical value. As long as the load is below this level the beam is stable and flexes in the plane of loading. When the critical load is reached the beam seeks a new equilibrium position. It deflects laterally and twists.

The critical load is dependent upon the properties of the beam cross section and the boundary conditions. The appropriate theory is well established. Prediction is in good agreement with experiment. Formulae have been developed for beams of common cross sections with simple loading and support conditions.

The case of a simply supported beam of narrow rectangular cross section is shown in Fig. 10(a). It is loaded at the centroid by a concentrated load which is free to move laterally by means of a ball and socket joint. The critical load is given by

$$P_{cr} = \frac{16.94\sqrt{EI_{\eta}C}}{L^2}$$

where I_{η} = principle moment of inertia of the cross section about the lateral bending axis.

C = torsional rigidity of the cross section.

L = length of span.

The mode of failure is depicted in Fig. 10(b).

As in the case of column members, the critical load may be increased by providing intermediate lateral supports. This causes a change in buckling mode and a corresponding increase in the buckling load.

Figure 10(c) shows the same beam in which the lateral movement of the load point has been prevented by removal of the swivel joint. This causes the second mode of lateral buckling to develope. Additional intermediate lateral supports would require a higher mode to develope and result in a substantial increase in the buckling load.

The circular cylindrical shell is one of the commonest elements in engineering use. For a century engineers have experimented with and theorized about its behavior under various loading conditions. The first theories for the buckling of thin-walled unstiffened circular cylinders were proposed by Southwell, Lorenz, and Timoshenko on the assumption of axisymmetric buckling. They deduced that the critical stress for such a shell with clamped ends was independent of the length of the shell and was given by the formula

$$\sigma_{cr} = \frac{0.6Et}{R}$$

The early experiments of Robertson and those of many engineers in the succeeding decades showed that these predictions were not consistent with reality. This classic buckling load is never achieved in practice and neither is the axisymmetric pattern.

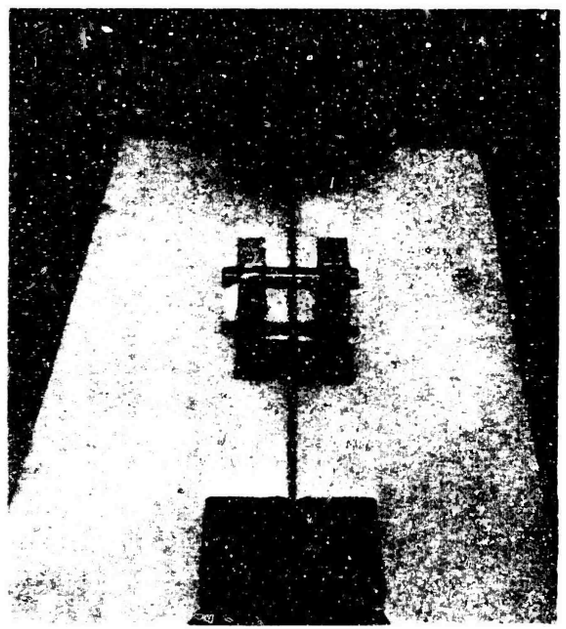

Fig. 10(a)--Beam Loaded Below Critical Load – Lateral Movement of Load Point Possible.

Fig. 10(b)--Buckling Mode – Lateral Movement of Load Point Possible.

Fig. 10--Lateral Buckling of a Long Narrow Rectangular Beam by a Concentrated Load Applied at the Centroid.

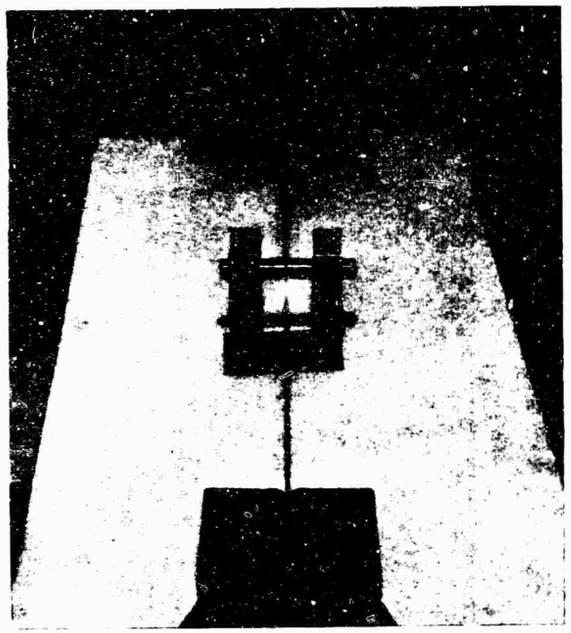

Fig. 10(c)--Beam Loaded Below Critical Load – Lateral Movement of Load Point Prevented.

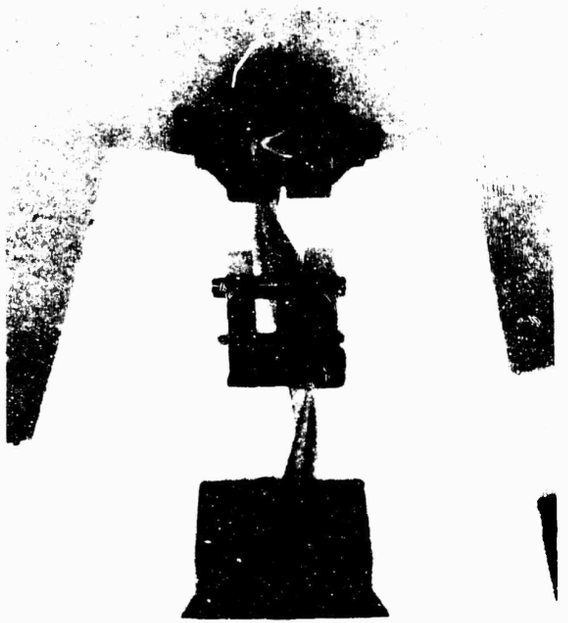

Fig. 10(d)--Buckling Mode – Lateral Movement of Load Point Prevented.

The buckles which occur are of a diamond character. As the pictures in Figs. 11(a-c) show, sometimes these buckles are located at the ends of the shell, sometimes in a ring around the center and in other cases they tend to form a spiral.

However it is clear, from analytical studies, that the discrepancy between calculated and observated loads is not due to the variation in buckle mode. The critical buckling load is remarkably insensitive to the buckle pattern used in the analysis. In 1934 Donnell proposed a nonlinear large displacement theory in which imperfections were considered and in which the buckle pattern was a square wave. While this was a step forwards, the problem still remained unsolved. There could be little doubt that imperfections caused a lowering of buckling load but it was apparent that they could not be identified and a rational theoretical solution given.

Almost a decade later, Kármán and Tsien developed the concept further and studied the postbuckling behavior of such bodies. Today, almost all work in the field is dominated by the Kármán-Donnell approach despite the fact that it does not agree any better with practical experience than the classic linear theory. Indeed, a very pertinent question can be asked -- is the designer interested in the minimum postbuckling or the maximum prebuckling load. There seems little doubt that it is the latter.

The Kármán-Donnell considerations are, however, such an integral part of current analytical thought that the tenets of this approach must be examined.

Initial buckling and postbuckling into the plastic range for flat plates in compression reflect an initially stable phenomenon with excellent correlation between theory and experiment. Cylinders and highly curved plates, however, exhibit an unstable initial buckling process with stability being achieved in the postbuckling range. It is classically contended that the stress at, and the nature of, the jump is greatly influenced by the method of application of the load for which there are two extreme possibilities:

(a) the rigid testing machine and

(b) the dead weight machine.

It is postulated that the total potential energy, (i.e., the sum of the strain energy and the potential energy of external forces) must be the same before and after the jump.

Fig. 11(a)--Edge Mode Buckle.

Fig. 11--Various Buckling Modes for Thin Circular Cylindrical Shells in Uniform Axial Compression.

Fig. 11(b)--Center Mode Buckle.
(Courtesy of Dr. R. L. Carlson, Stanford University)

Fig. 11(c) -Spiral Mode Buckle.

Symbolically $U = K\left(\int \sigma d\epsilon - \sigma\epsilon\right) = -K\int \epsilon d\sigma = \text{const.}$

In a rigid test machine the jump occurs at constant end shortening while in a dead weight machine it is at constant stress. These considerations lead to the situation depicted in Figs. 12(a,b). The analytical logic is hard to decry – but experiment indicates that the argument must be false. No significant difference in behavior can be determined no matter what machine stiffness is used.

Researchers today, working in both the analytical and experimental fields are still attempting to unravel this most perplexing problem. It has been found that if the depth to which buckles are developed is restricted by an internal mandrel a shell can be completely filled with buckles. These buckles are diamond in shape and produce a very regular pattern as shown in Fig. 13. They occur in a random sequence as the loading cycle is carried through and some occur at a lower and some at a greater level of load than would be predicted on the classic theory. In fact, the population of buckles is described by a normal population law and the point of maximum buckle generation corresponds to the classic critical load. This particular experiment demonstrates that a perfect shell restricted to operate within the confines of the small displacement theory will buckle at the predicted stress level.

Perfection, of course, is not achievable either in material characteristics, in geometric form or in the loading system. The question which confronts the engineer is to what extent do these various imperfections influence the situation either individually or in combination.

There are several aspects which are readily demonstrated. First, in buckling of shells and curved plates plastic deformation occur at the folds of the buckles even when the deformation is very small, say no more than twice the thickness of the shell. A consequence of these very early plastic stresses is that on repeated testing the load to produce instability falls off. Second, the character of the buckles produced by nonsymmetric distributions of load is the same as that which results from uniform compression. This is clearly seen in the sequence of pictures, Fig. 14. It can be experimentally demonstrated that the critical stress required to produce instability is the same whether the distribution is uniform or not.

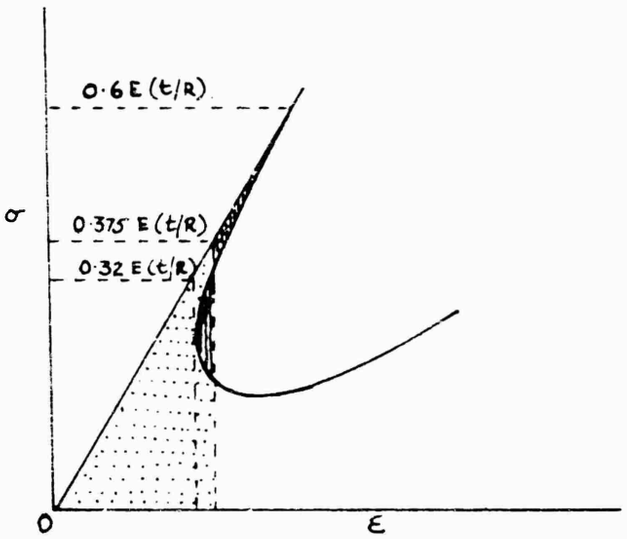

(a) RIGID TEST MACHINE CASE

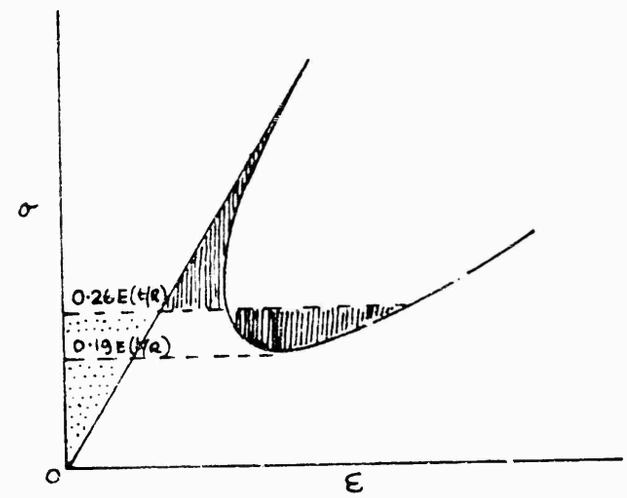

(b) DEAD WEIGHT MACHINE CASE

Fig. 12--Buckling of a Thin Circular Cylindrical Shell in Axial Compression – Rigid Test Machine Case Fig. 12(a) – Dead Weight Machine Case Fig. 12(b).

Fig. 13--Cylinder With Completely Developed Elastic Buckle Pattern.
(3 in. O.D., 9 in. length and 0.004 in. thickness, nickel)

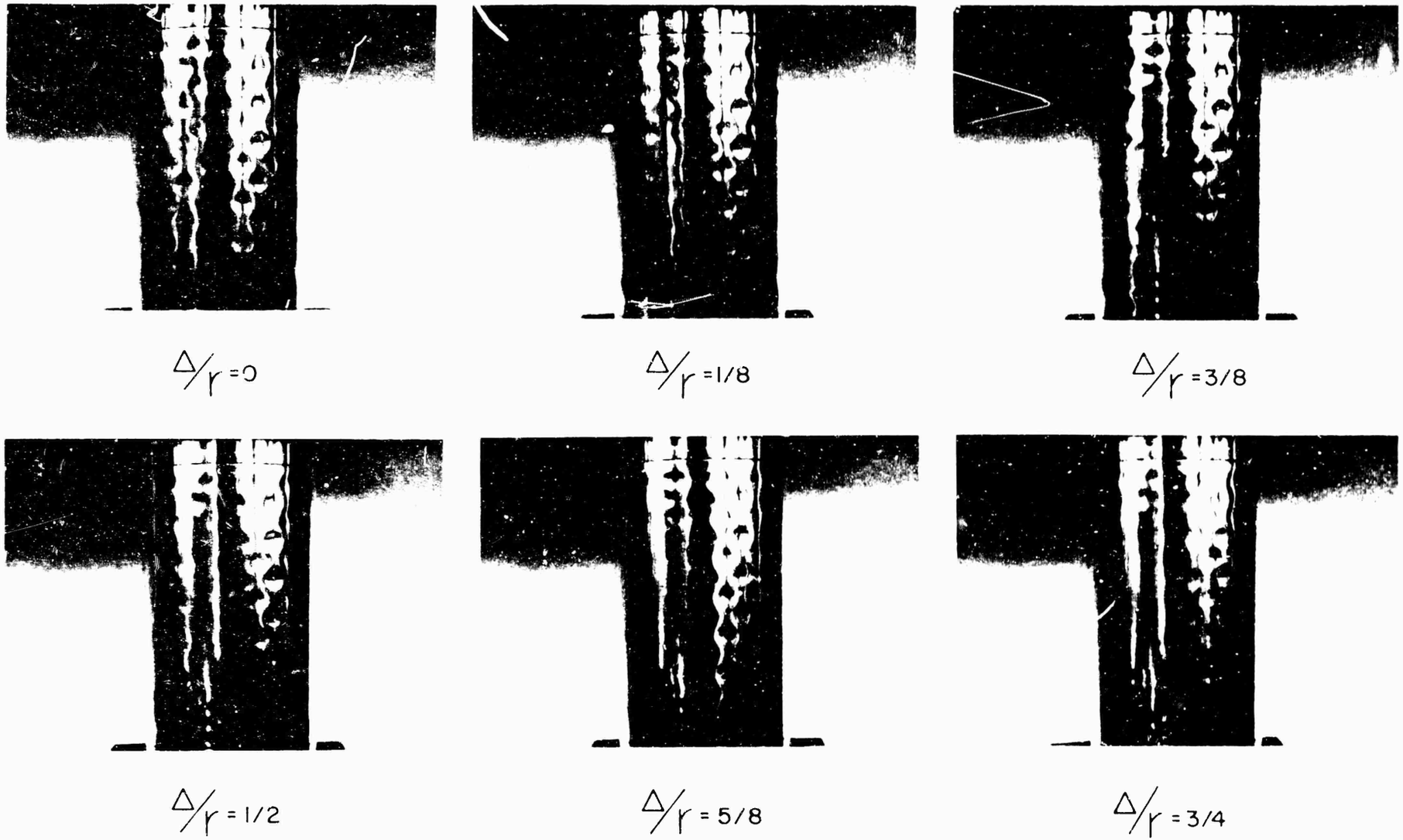

Fig. 14--Buckle Population for Various Eccentric Positions of the Axial Load

So far the precise effect of variation in geometry of the shell has not been established. Analytically and experimentally, however, it is possible to demonstrate that boundary conditions are of extreme importance to the behavior. Changes at this point can very easily reduce the achievable stress by 50 per cent.

The behavior of anisotropic shells, such as are common in plywood, fiber reinforced materials and so on is not easier to deal with than the isotropic case already discussed. There seems to be some doubt whether fiber direction influences stability loads for thin-walled bodies. Experiments with cylinders made of a fiber material of close weave which had approximately the same character in the direction of weft and warp indicated no dependence of load on fiber direction. There is no doubt, however, that in thicker walled shells such as those made from sandwich materials, imperfections are less important even when the R/t would still cause them to be classed as thin-walled. However, the boundary conditions in sandwich shells are much more complex than those in isotropic bodies.

The conical shell buckles in much the same manner as the cylinder. The pictures of Figs. 15(a,b) illustrate this. The same difficulties are present— imperfection of load distribution, boundary and geometry give serious scatter.

The behavior of cylindrical shells under the action of combined internal pressure and direct load is analytically ill defined. There is little doubt that the presence of internal pressure does increase the load level required to produce instability for a realistic shell. There seems to be little question that for a perfect shell there would be no influence. Tests are characterized by much scatter and by a variation in buckle shape. The shape of the buckle is dependent upon both the value of the compressive stress and the level of the internal pressure. As the pressure increases the buckle aspect ratio, the ratio of wavelength to height — increases until at some critical value of internal pressure axisymmetric buckling occurs. This is clearly evident in the sequence of shots shown in Figs. 16(a-c). The tendency to spiral is also more predominant in internal pressure-compression behavior than in pure compression. A spiral pattern is shown in Fig. 16(d).

Axisymmetric buckles — ring buckles are quite clearly extensional deformation patterns whereas for diamond shapes inextensional deformation is possible. Yoshimura has shown that a circular cylinder can deform in an

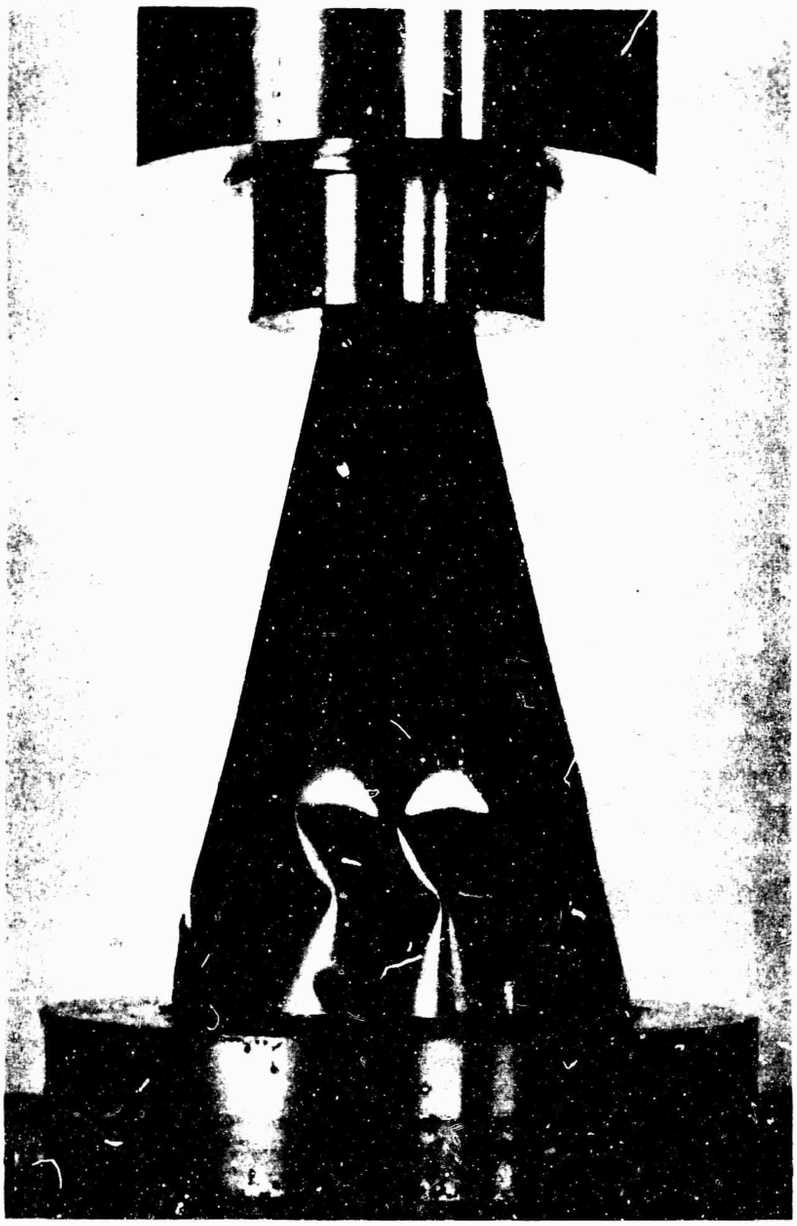

Fig. 15(a)--Edge Buckle Pattern
(Courtesy of Dr. R. L. Carlson, Stanford University)

Fig. 15--Typical Buckle Pattern for a Thin-Walled Conical Shell in Axial Compression.

Fig. 15(b)--Buckle Pattern Almost Completely Developed.

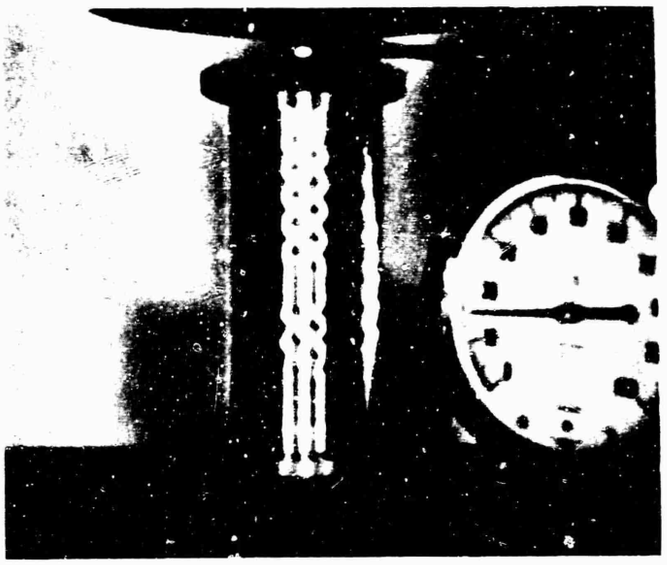

Fig. 16(a)--Buckle Pattern With 15 psi Internal Pressure.

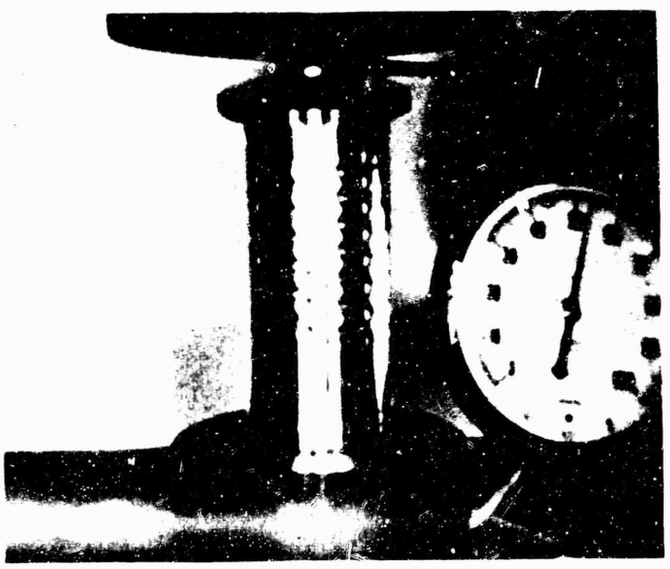

Fig. 16(b)--Buckle Pattern With 54 psi Internal Pressure – Just Prior to Jumping Into a Single Plastic Ring.

Fig. 16--Variation in Buckle Aspect Ratio With Combined Internal Pressure and Axial Compression.

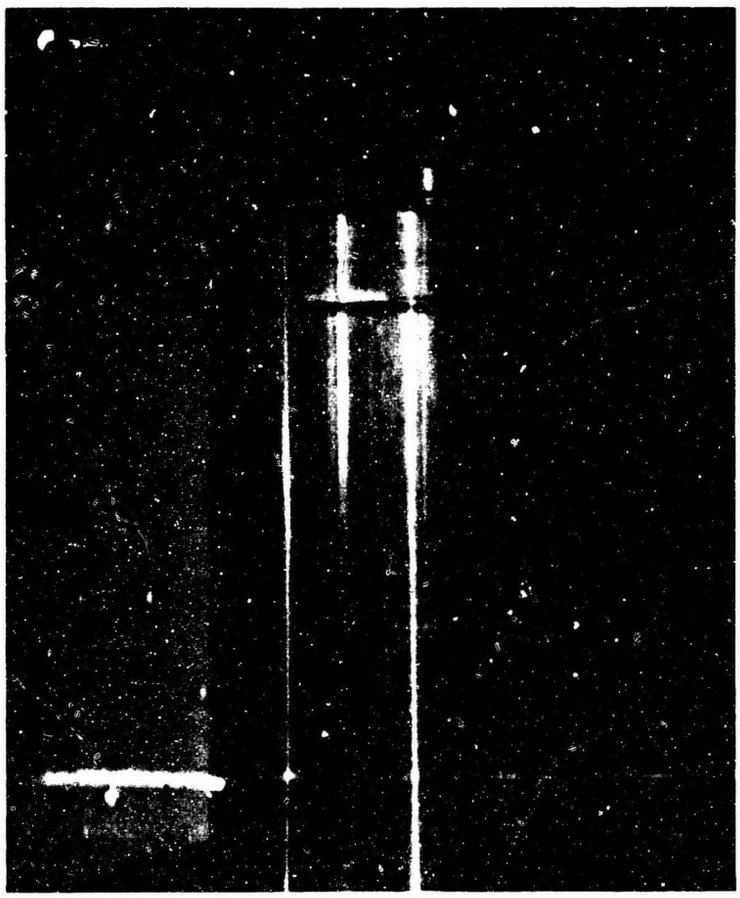

Fig. 16(c)--View of Plastic Ring Failure at 55 psi Internal Pressure.

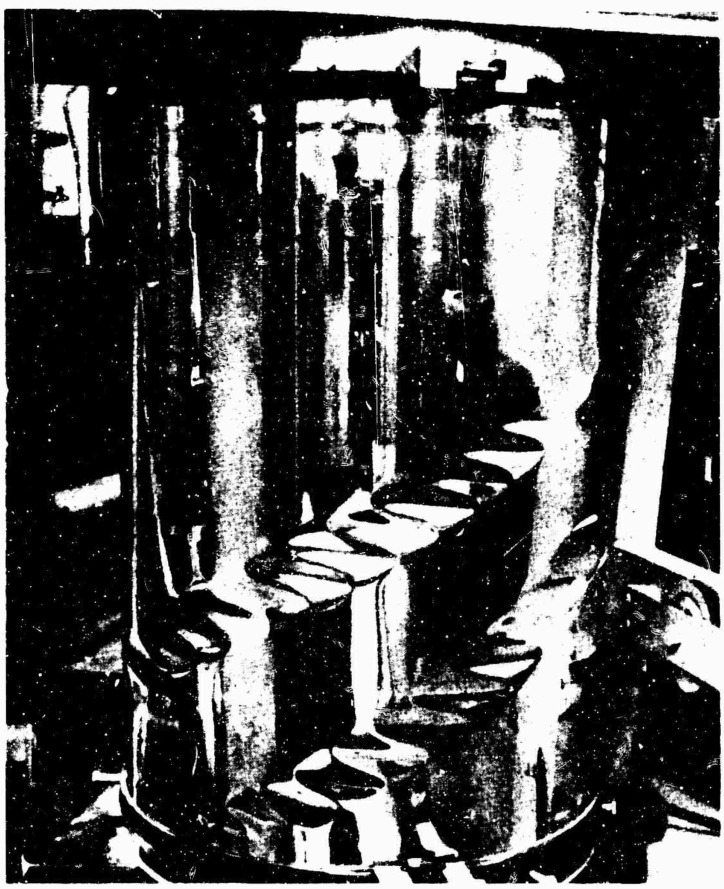

Fig. 16(d)--View of Elongated Buckle Shape in Spiral Mode Pattern.

(Courtesy of L. A. Harris, et al, Experimental Mechanics, July 1961)

inextensional manner and become completely filled with a pattern made up from flat sided figures. In practice this is very difficult to achieve unless there are hinge lines present in the shell. That it can result in this case is clear from Figs. 17(a,b). This inextensional deformation pattern seems to be the limiting case of what is likely to occur when the predominant load condition is compression.

The buckling behavior of cylindrical shells under torsion is illustrated in Figs. 18(a,b) and under combined pressure and torsion loadings in Figs. 18(c-e). For the case of buckle depth restriction the torsion buckle pattern is depicted in Figs. 18(f-i). The buckles are very different from those seen in compression. In fact they are somewhat reminiscent of those for the tension field. For instability under torsion, theory and experiment are much more in consonance than for the case of compression loading. The correlation factor between calculated and observed is of the order 0.60 whereas in compression it is more nearly 0.20.

The theoretical values for the critical shear stress are given by

$$\tau_c = \frac{Et^2}{(1-\mu^2)L^2}\left[4.6 + \sqrt{7.8 + 1.67\left(\sqrt{1-\mu^2}\,\frac{L^2}{td}\right)^{3/2}}\right] \quad \text{for clamped ends.}$$

$$\tau_c = \frac{Et^2}{(1-\mu^2)L^2}\left[2.8 + \sqrt{2.6 + 1.4\left(\sqrt{1-\mu^2}\,\frac{L^2}{td}\right)^{3/2}}\right] \quad \text{for simple}$$

support.

The influence of external pressure on the stability of a circular cylinder is a subject which has received much attention. The agreement between experiment and theory is good. Under these conditions the critical loads and lobe numbers are dependent upon the ratio of the thickness to diameter and the specimen length. Buckle patterns for thin-walled cylinders are shown in Figs. 19(a,b).

Spheres, spherical domes and caps find much application in engineering. Generally speaking, there is wide disagreement between the predictions of theory and the experimentally observed behavior for thin-walled shells. There seems little doubt that such bodies are seriously influenced by imperfections particularly when loaded under uniform external pressure. In thin-walled

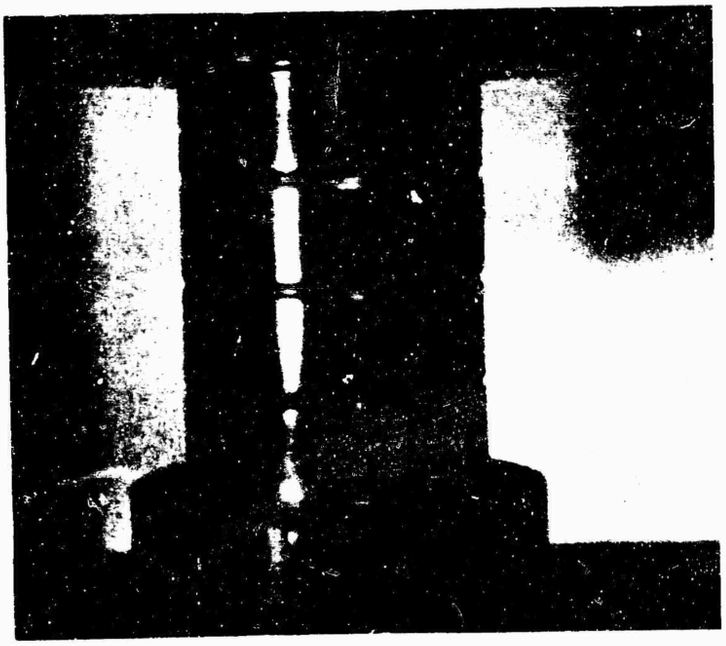

Fig. 17(a)--Cylinder With Evenly Spaced Hinge Lines Prior to Buckling.

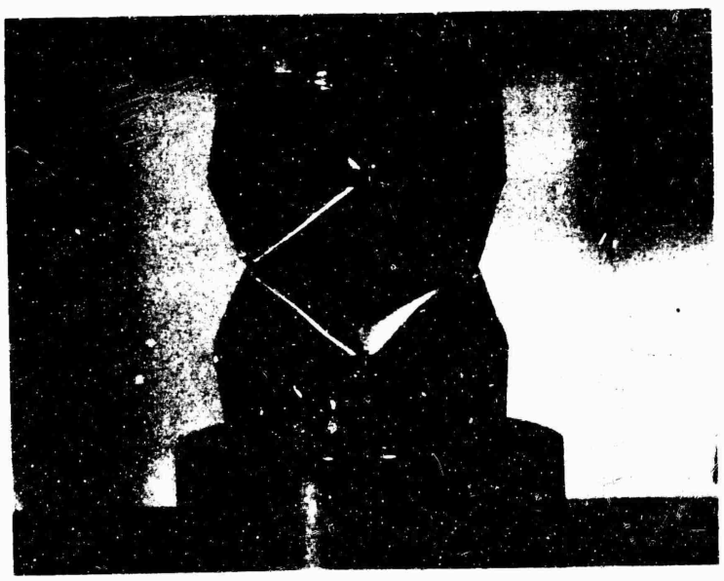

Fig. 17(b)--Yoshimura Pattern Fully Developed.

Fig. 17--Yoshimura Buckling Pattern Developed in a Circular Cylindrical Shell in Axial Compression.

Fig. 18(a)--Typical Buckle Pattern for Unpressurized Cylinder in Torsion. (Courtesy of L. A. Harris, H. Suer, W. Skene – Experimental Mechanics, July 1961)

Fig. 18--Torsional Buckling of Thin Circular Cylindrical Shell.

Fig. 18(b)--Typical Buckle Pattern for Stainless Steel Cylinder Under Torsional Loading. (Courtesy R. E. Ekstrom, Experimental Mechanics, August 1963)

Fig. 18(c)--Ripples in Pressurized Specimen Prior to Buckling.
(Courtesy L. A. Harris, et al)

Fig. 18(d)--Typical Buckle Pattern for Pressurized Cylinder in Torsion. (Courtesy L. A. Harris, et al)

Fig. 18(e)--Typical Buckle Pattern for Combined Torsion and External Pressure. (Courtesy L. A. Harris, et al)

Fig. 18(f)--Torsional Buckling Pattern of a Short Cylinder When Depth of Buckle is Restrained by an Internal Mandrel.

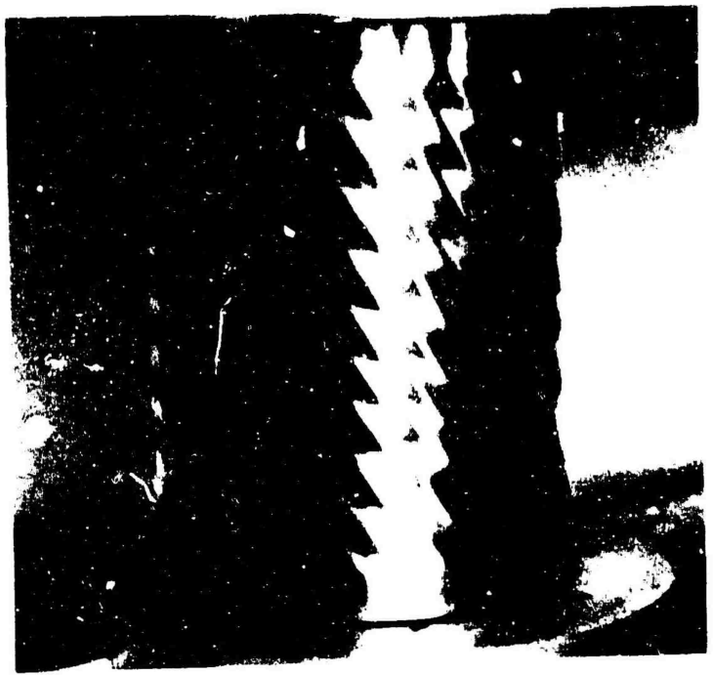

Fig. 18(g)--Change in Buckle Pattern as Torque is Increased.

Fig. 18(h)--Torsional Buckling Pattern of a Long Cylinder When Depth of Buc[illegible]s Restrained by an Internal Mandrel.

Fig. 18(i)--Change in Buckle Pattern as Torque is Increased.

Fig. 19(a)--Typical Buckle Pattern for Stainless Steel Cylinder Under Hydrostatic Loading. (Courtesy R. E. Ekstrom, et al)

Fig. 19--Buckling of a Thin-Walled Circular Cylindrical Shell Under External Pressure.

Fig. 19(b)--Typical Multilobe Buckle Pattern for Hydrostatic Pressure. (Courtesy L. A. Harris)

spherical shells loaded in this fashion the implosion is very dynamic and the buckle behavior which results is seen in the photograph of Fig. 20. The development of the buckle motion is hard to follow even with extremely high framing rate cameras.

If the buckling motion in such a shell loaded by external pressure is restrained by an interior mandrel buckling begins as a series of circular indentations which grow in size, coalesce together and in so doing form a system of hexagons and pentagons as seen in Figs. 21(a-c). This buckle pattern is a very interesting one. It bears a very remarkable similarity to the structure of a marine organism – the radiolarian. Plastic stresses occur in the folds of the buckles just as in the case of cylinders but the deformation which can exist before they develope seems to be a good deal larger.

It is apparent from Fig. 22 that when a thin-walled sphere is compressed by a force normal to its surface, buckling will take place in the neighborhood of the force. It is not so immediately apparent that this also occurs when tensile loads are applied to the shell either tangential to it or normal to it. The pictures, Figs. 23(a-g), show spherical shells subjected to various loading conditions. The buckle patterns are illustrative of a very important aspect in instability considerations, viz., it is not the nature of the applied force which is important but the nature of the reactive distribution of stress.

Thus, we can find examples of instability under internal pressure. For example, cylindrical pressure vessels in which the end cap is not spherical can be unstable structures. This is illustrated in Figs. 24(a-b).

Naturally, all structures are not thin-walled. Thick-walled cylinders, for example, find much application in engineering. The discussion now turns to a consideration of such vehicles; cylinders in which the radius-to-thickness ratio is measured in tens rather than in hundreds or thousands. This problem is just as difficult from an analytical point of view as many of the questions which have been discussed previously. The classic buckling behavior is of the axisymmetric ring type. This is, as previously remarked, an extensional type of deformation and there is clear evidence when thick-walled shells buckle in this fashion that the material yields along the fold lines. According to current theory, nonsymmetric buckling should require a higher load level to produce it. Nevertheless, in practice this is not always

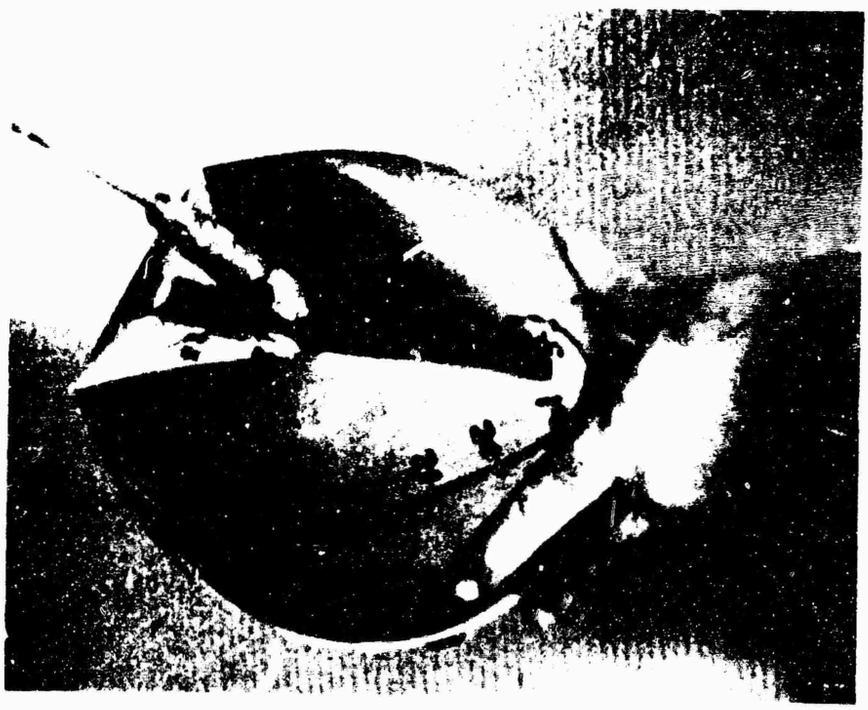

Fig. 20--Buckling of a Thin-Walled Spherical Shell Loaded With Uniform External Pressure.

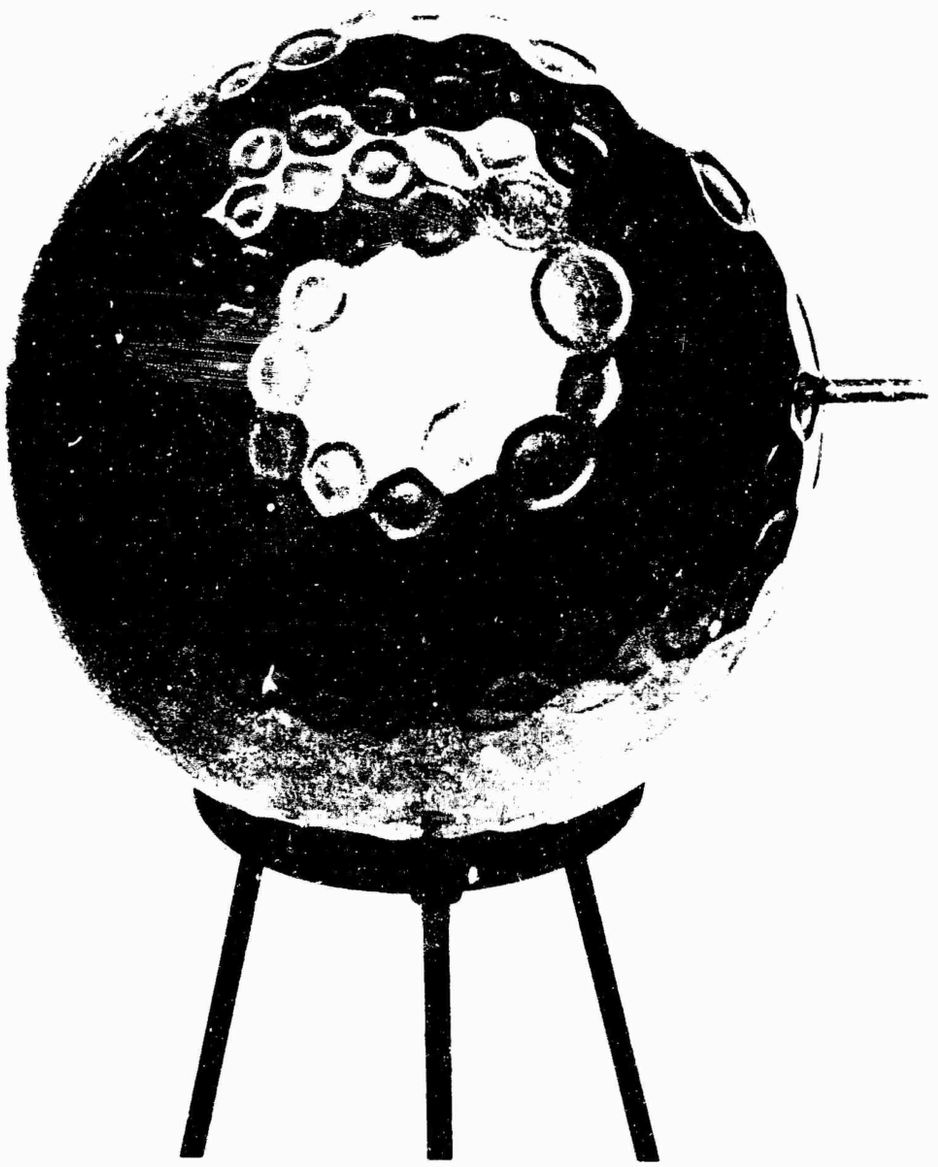

Fig. 21(a)--Completely Developed Buckle Pattern.

Fig. 21--Buckling of a Thin-Walled Spherical Shell Loaded With Uniform External Pressure When Buckling Motion is Restrained by an Interior Mandrel.

Fig. 21(b)--Close-Up View of Buckle Pattern.

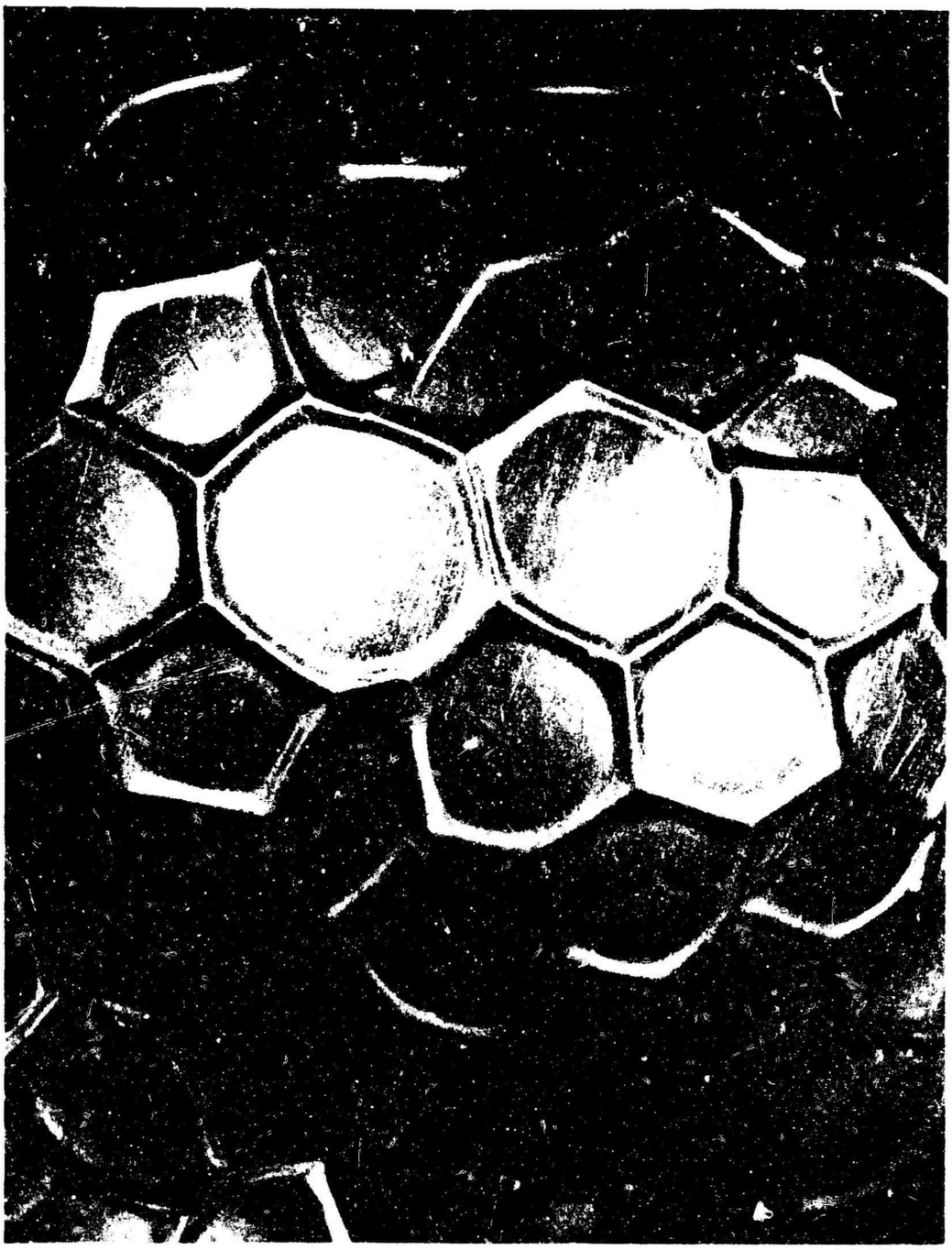

Fig. 21(c)--Close-Up View of Final Buckle Pattern.

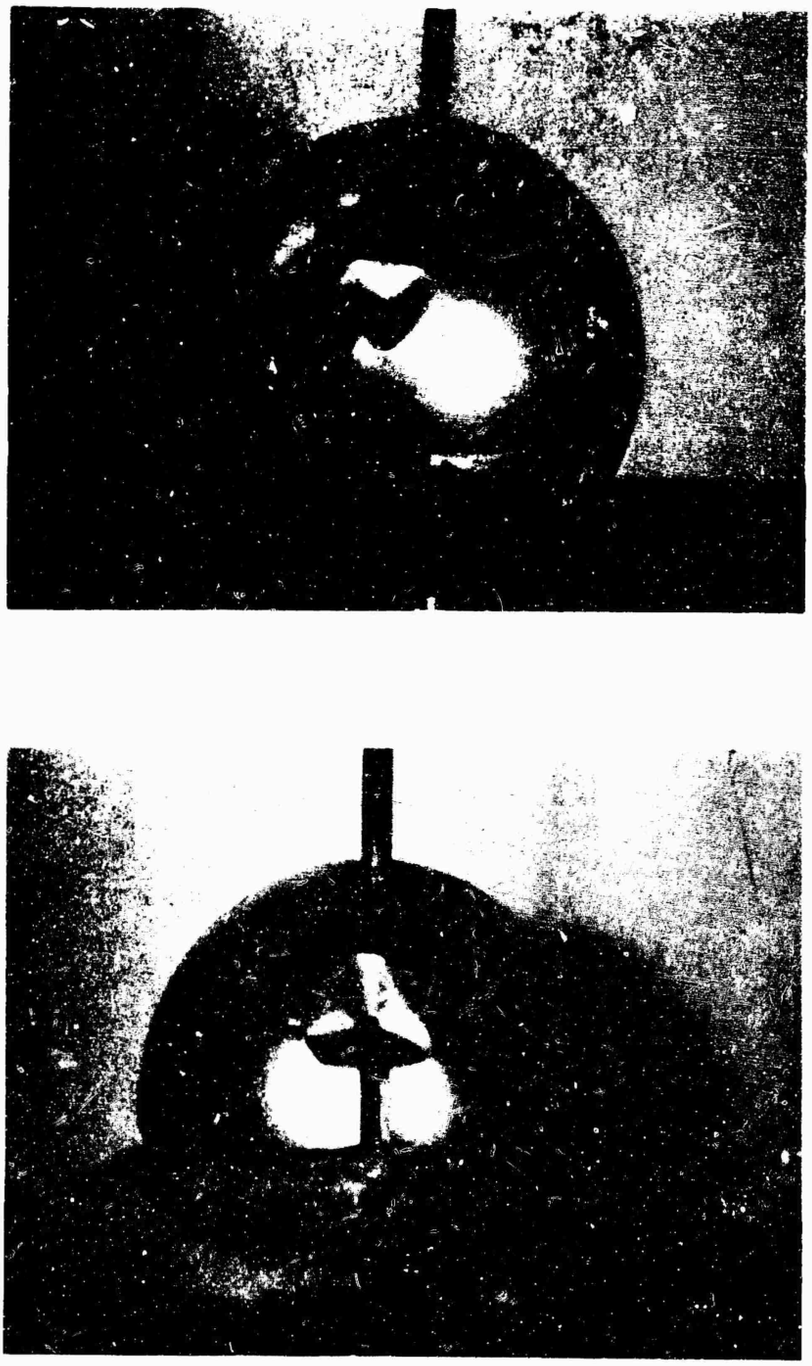

Fig. 22--Buckling of a Thin-Walled Spherical Shell by a Force Normal to its Surface.

Fig. 23(a)--Buckle Pattern – Normal Tensile Force.

Fig. 23--Buckling Patterns for Thin Spherical Shells Subjected to Various Loading Conditions When Buckle Motion is Restrained by an Interior Mandrel.

Fig. 23(b)--Buckle Pattern – Normal Tension Force With External Pressure.

Fig. 23(c)--Buckle Pattern - Normal Tension Force After Release of External Pressure.

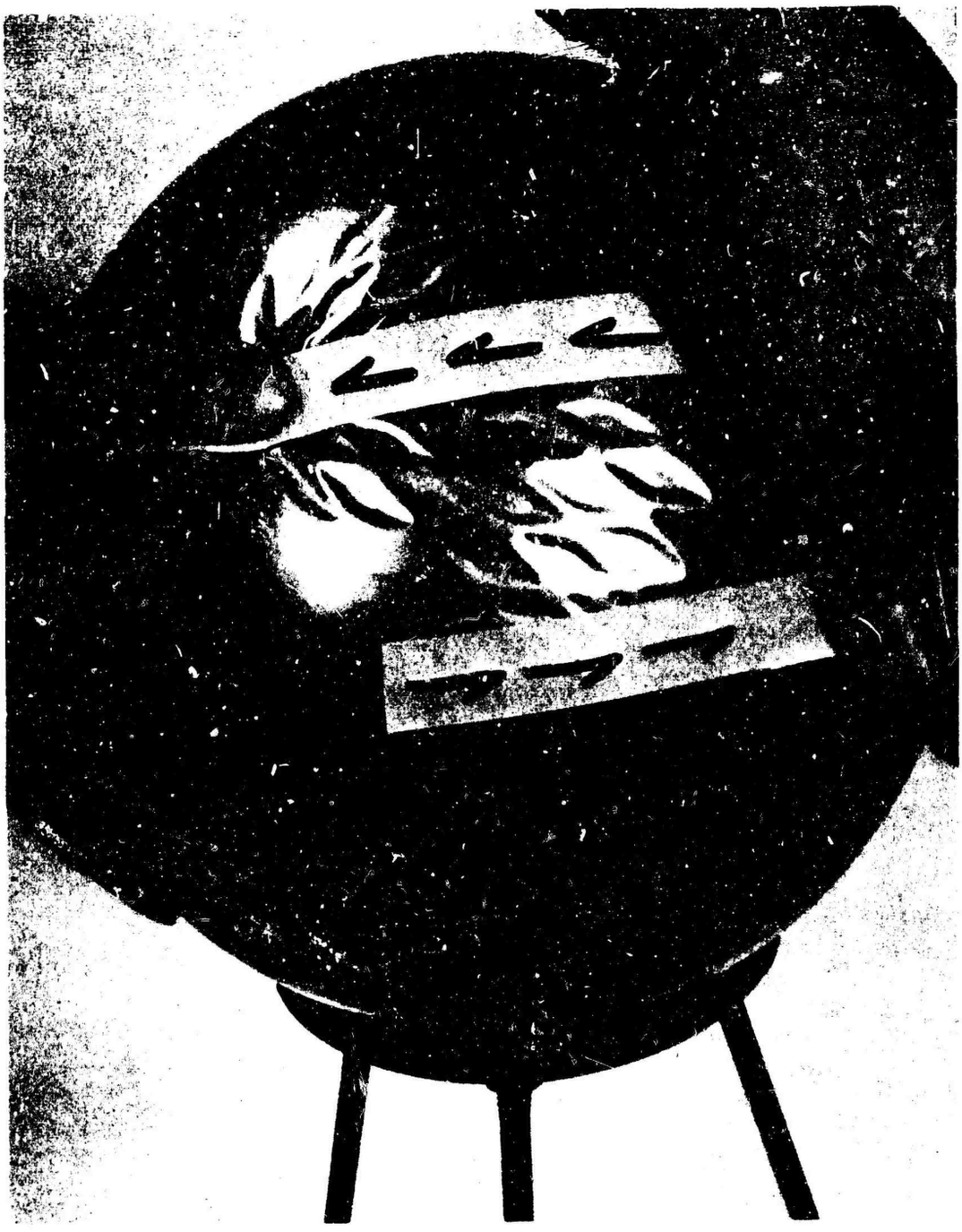

Fig. 23(d)--Buckle Pattern – Surface Shear Force.

Fig. 23(e)--Buckle Pattern – Surface Tension Force.

Fig. 23(f)--Buckle Pattern – Two Perpendicular Surface Tension Forces.

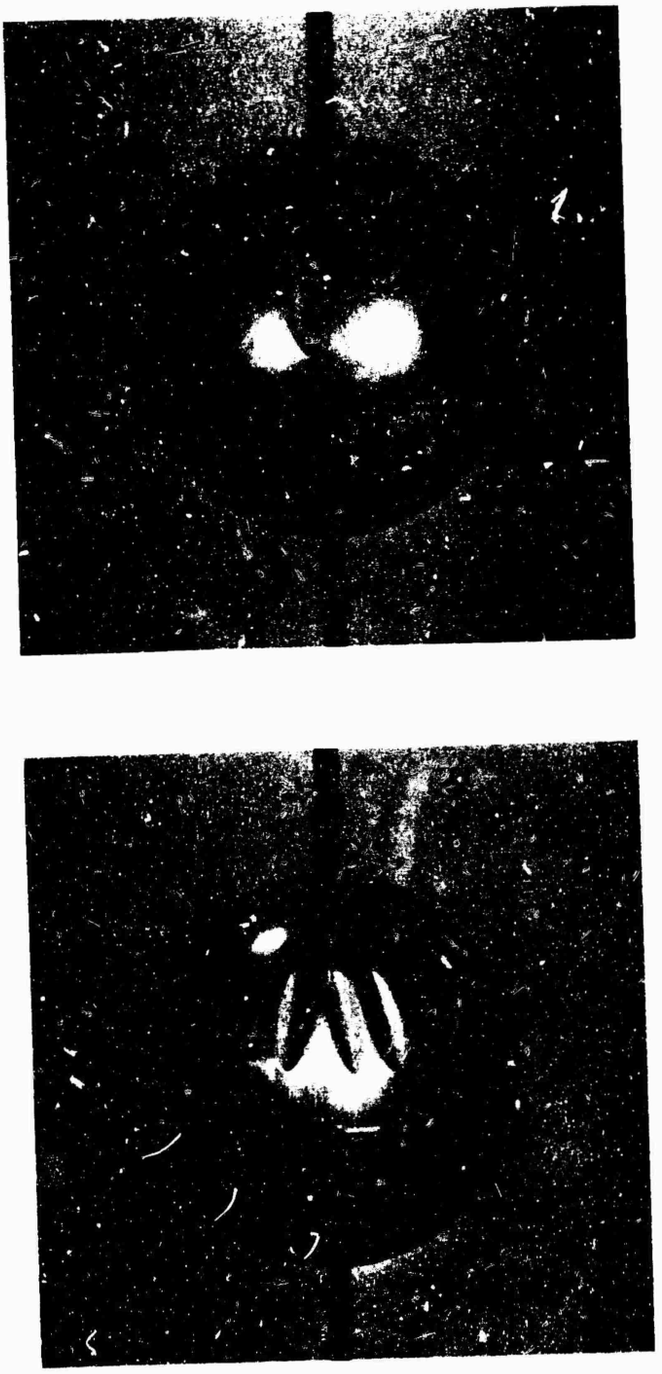

Fig. 23(g)--Buckling Pattern for a Thin-Walled Spherical Shell With a Solid Bottom Half and Tension Applied by Means of an Internal Spherical Cap.

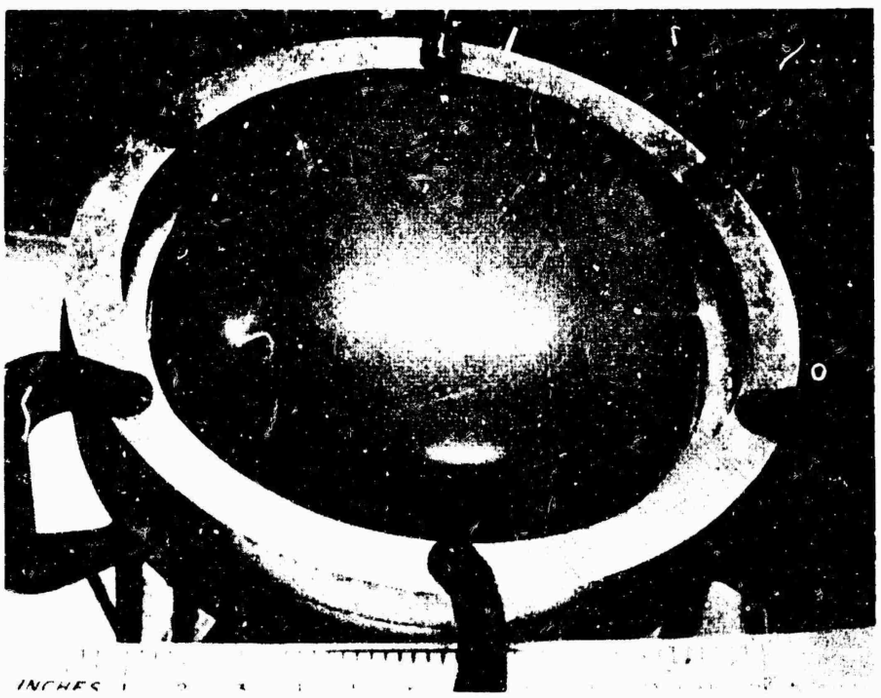

Fig. 24(a)--Initial Buckle.

Fig. 24--Instability Under Internal Pressure of a Nonspherical End Cap. (Courtesy J. Adachi and M. Benicek, Experimental Mechanics, July 1964)

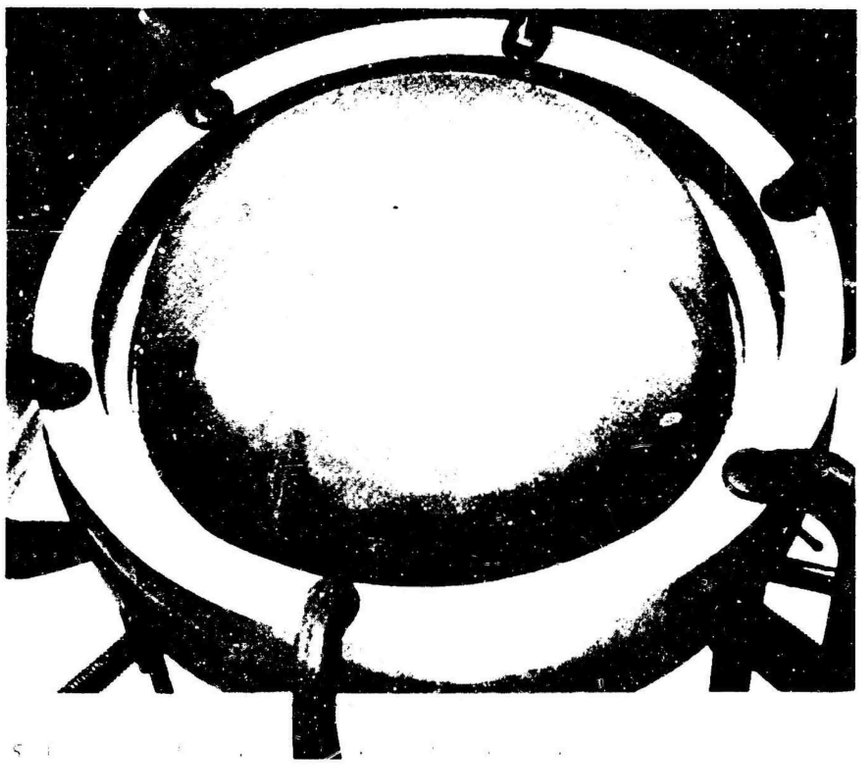

Fig. 24(b)--Additional Buckling.

found to be the case. Much more complex buckling patterns can and do exist. Some of these are shown in the photographs of Figs. 25(a-i). Herein demon strated are buckle types in which the rings have become elliptical in character, a case in which the ellipses have become almost orthogonal rectangles together with examples of 2, 3, and 4 lobe buckles. There is a great similarity between these multilobe patterns and the Yoshimura pattern which we previously discussed. This is very clearly seen in the photographs. In buckling of this kind the material flows very much like a viscous fluid.

The "geodetic shell" is a form which seems to have increased potential. So far as can be traced there is no current literature which deals with the stability of cylinders of this type under axial compression. Civil engineers, of course, have considered reticular domes under normal force and radar housing under wind loadings. Axial compression tests have shown that for such bodies made from relatively thick materials some very interesting buckle deformations are possible. In some cases there is a distinct analogy between the behavior of this type of structure and thick-walled shells but there are also deformation patterns with no counterpart in normal shell bodies. In Figs. 26(a,b) the deformations are seen to be very similar to the classic axisymmetric ring deformation. The behavior pattern portrayed in Figs. 26 (c-f), is, however, very different. Here the shell is seen to almost turn inside out. The situation portrayed in Figs. 26(g-h) is again somewhat unusual since the failing mode is of the torsional type. In Figs. 26(i-k) other unusual modes are illustrated.

This broad but elementary survey of the instabilities of bars, plates, and shell bodies has served to illustrate that the field of structive instability is most complex and perplexing. There is a clear need for research of theoretical and experimental kinds to help unravel the many questions. There is need in all experimental studies for an awareness that boundary conditions are of paramount importance and must be carefully controlled. The state-of-the-art is a clear indication that we should pay heed to the remark made by Dr. Johnson

> "The mathematicians are well acquainted with the difference between pure science, which has to do only with ideas, and the application of its laws to the use of life, in which they are constrained to submit to the imperfections of matter and the influence of accident."

There seems little doubt that the imperfections of matter and the influence of accident are of extreme importance in all phases of the very difficult field.

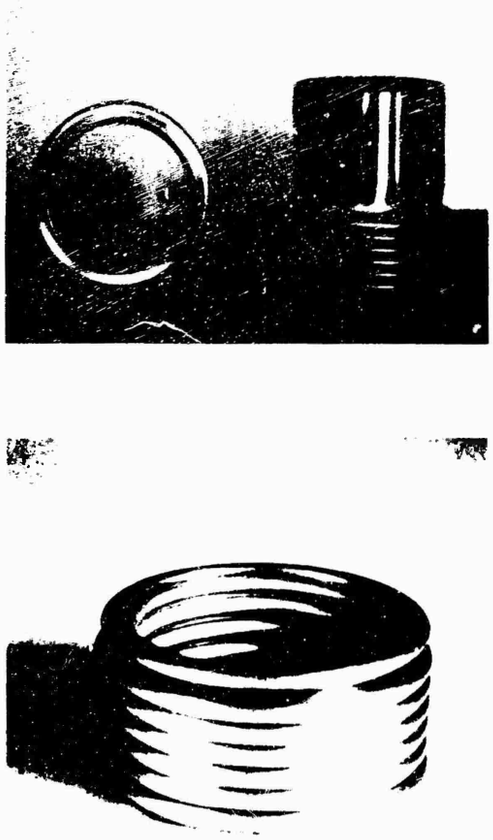

Fig. 25(a)--Symmetric Ring Buckles.

Fig. 25--Symmetric and Nonsymmetric Buckle Patterns in Progressive Plastic Buckling of Circular Cylindrical Shells.

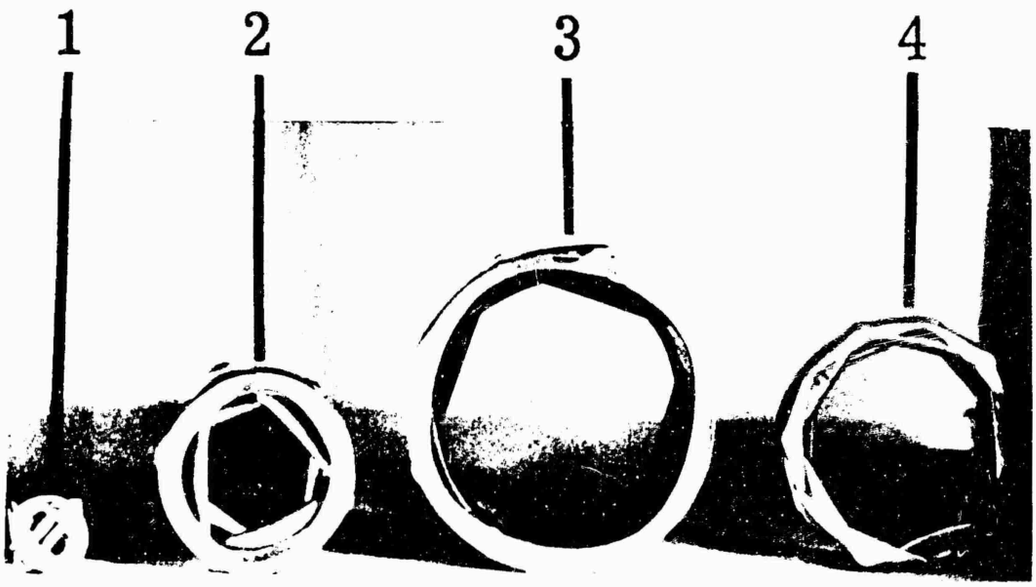

Fig. 25(b)--End View of Nonsymmetric Buckle Patterns.
1. Two-Lobe Failure
2. Three-Lobe Failure
3. Four-Lobe Failure
4. Five-Lobe Failure

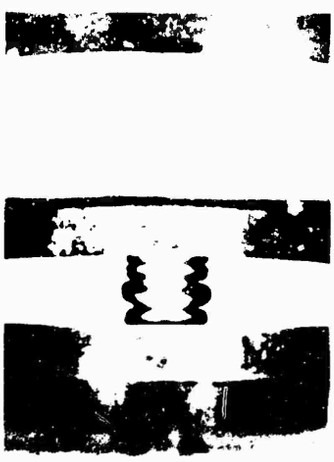

Fig. 25(c1)--Collapsed Specimen.

Fig. 25(c2)--End View Showing Elliptic Cross Sections With Layer by Layer Rotations.

Fig. 25(c)--Elliptic Cross Section Buckles.

Fig. 25(d1)--Collapsed Specimen.

Fig. 25(d2)--End View Showing Fold Line With Layer by Layer Rotation.

Fig. 25(d)--Two-Place Buckle Pattern.

Fig. 25(e1)--Collapsed Specimen.

Fig. 25(e2)--End View Showing Triangular Cross Sections With Layer by Layer Rotation.

Fig. 25(e)--Three-Lobe Buckle Pattern.

Fig. 25(f1)--Collapsed Specimen.

Fig. 25(f2)--End View Showing Square Cross Sections With Layer by Layer Rotation.

Fig. 25(f)--Four-Lobe Buckle Pattern

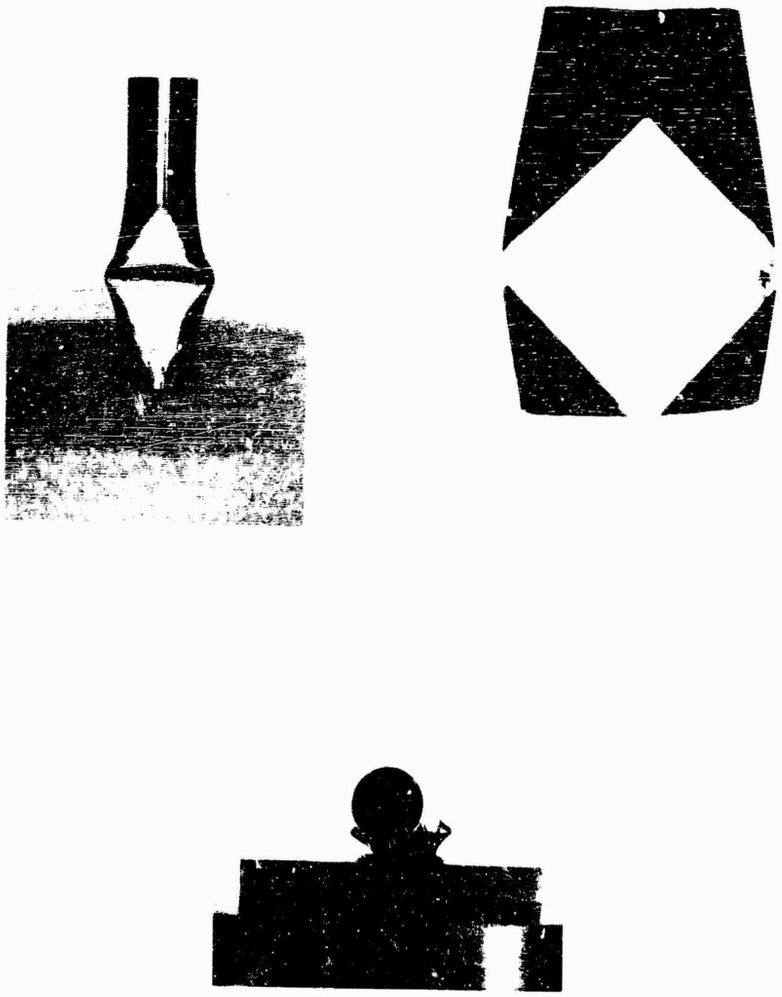

Fig. 25(g)--Two-Lobe Failure and Yoshimura Model.

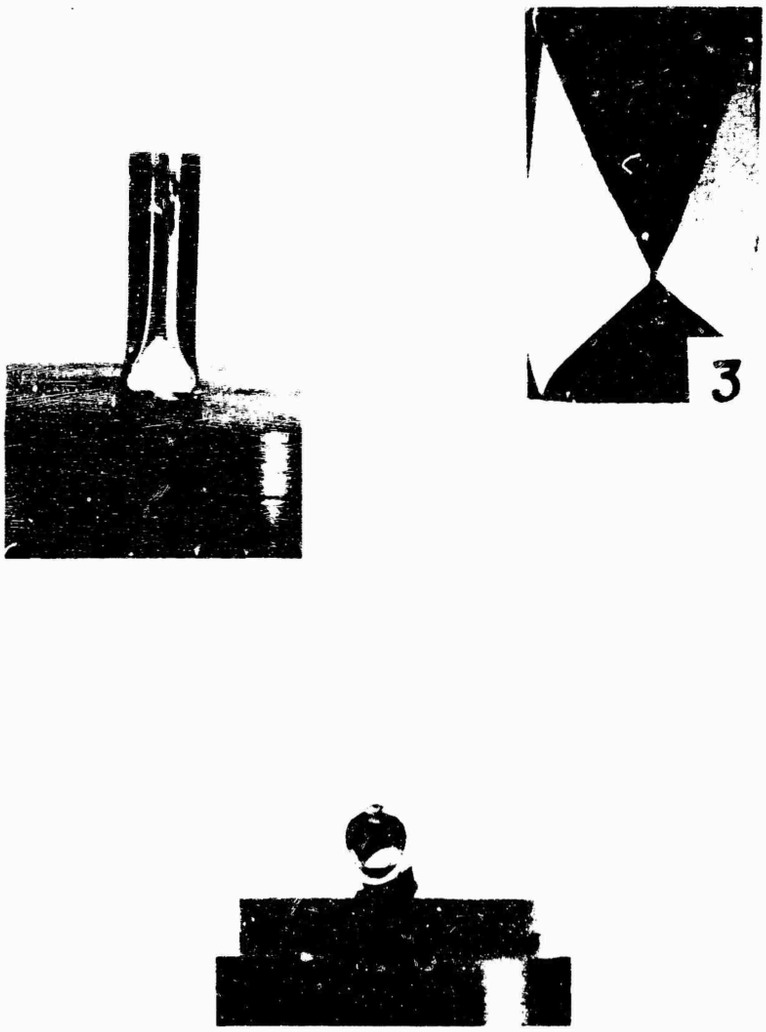

Fig. 25(h)--Three-Lobe Failure, End View and Yoshimura Model.

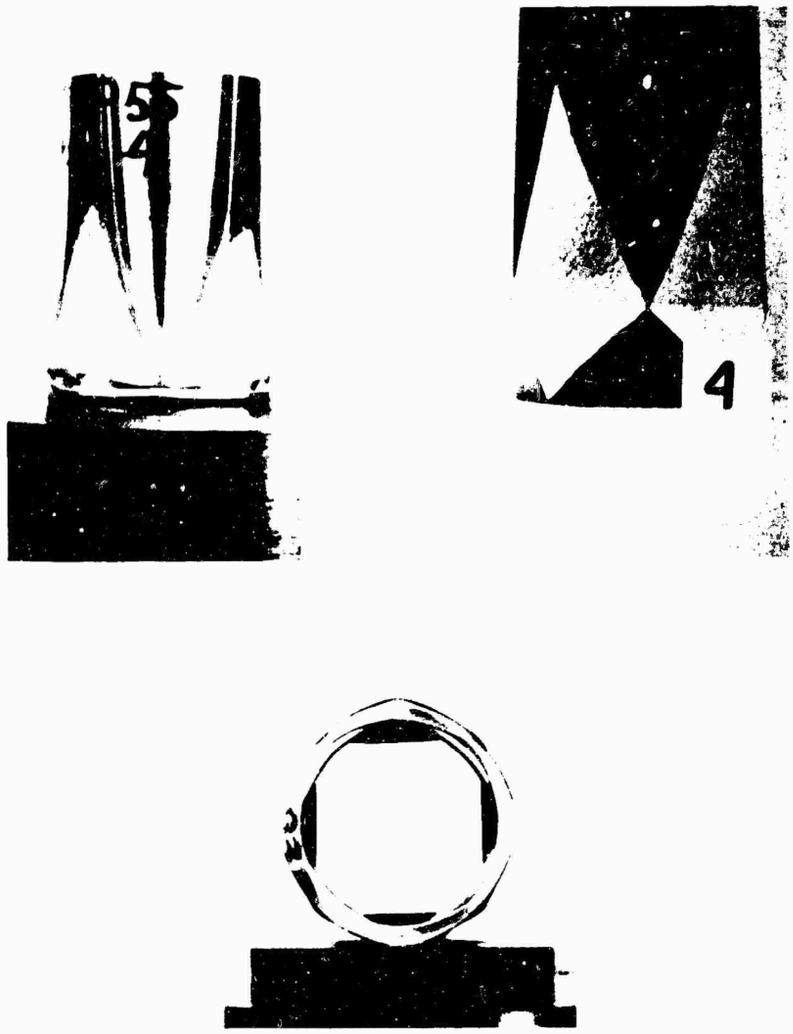

Fig. 25(i)--Four-Lobe Failure, End View
and Yoshimura Model.

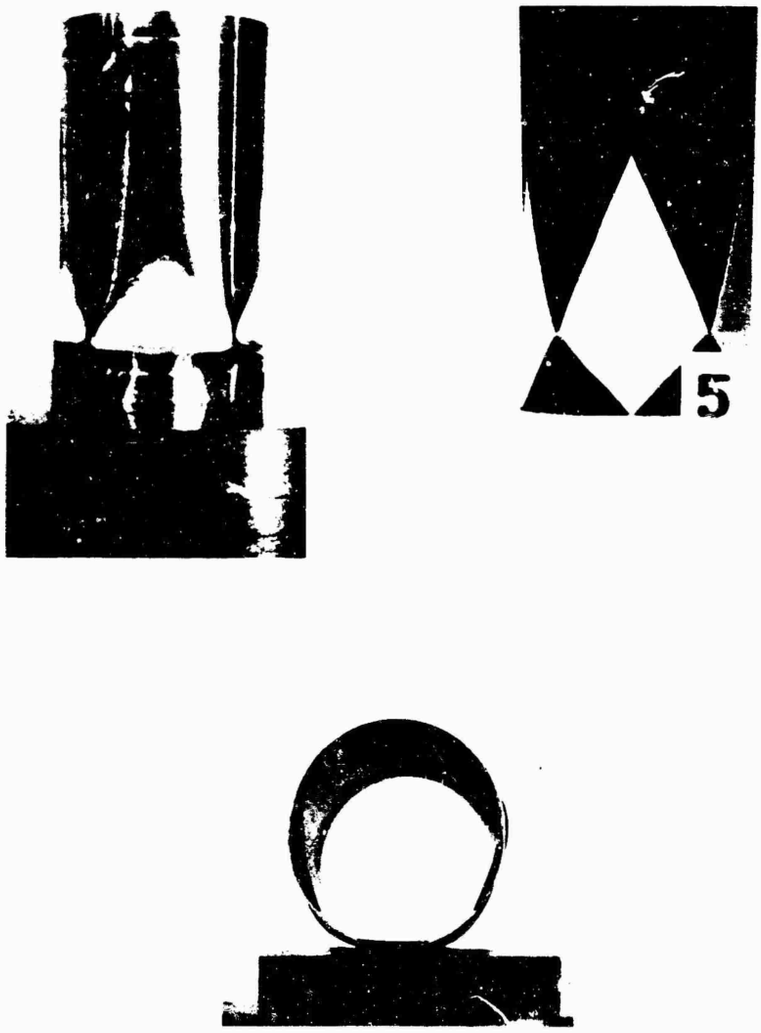

Fig. 25(j)--Five-Lobe Failure, End View and Yoshimura Model.

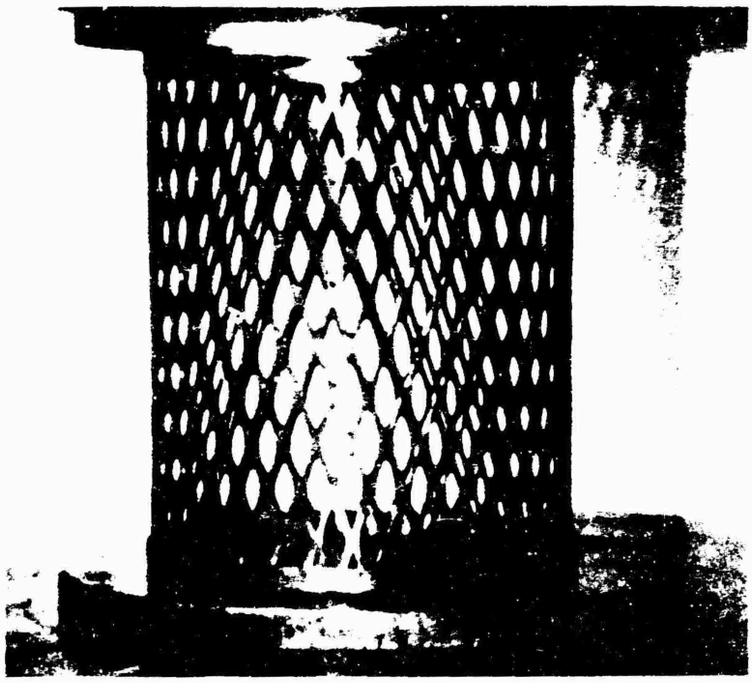

Fig. 26(a)--Short Specimen With Vertical Orientation of Diamond Patterns.

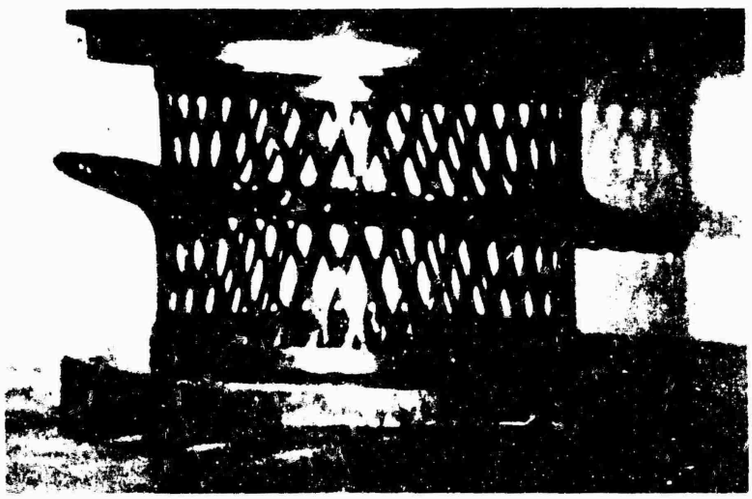

Fig. 26(b)--Collapsed Specimens – Hat Mode.

Fig. 26--Symmetric and Nonsymmetric Buckle Patterns in Plastic Buckling of Perforated Circular Cylindrical Shells.

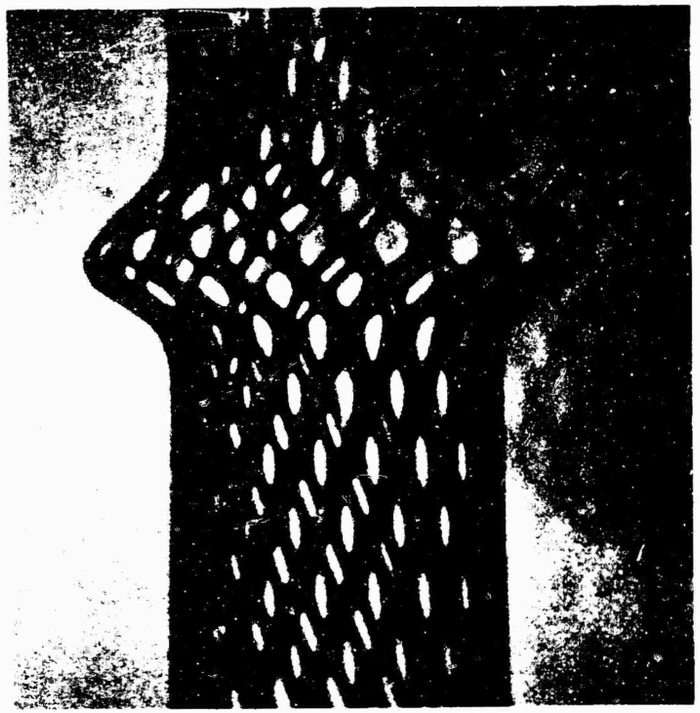

Fig. 26(c)- -Long Specimen With Vertical Orientation of Diamond Pattern – Initial Collapse Ring.

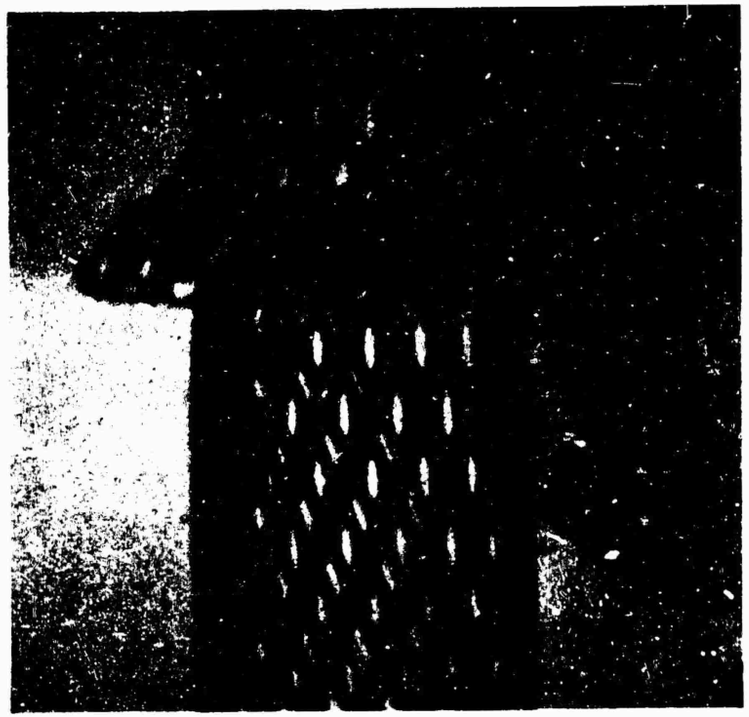

Fig. 26(d)--Additional Collapse.

Fig. 26(e)--Advanced Stage of Collapse.

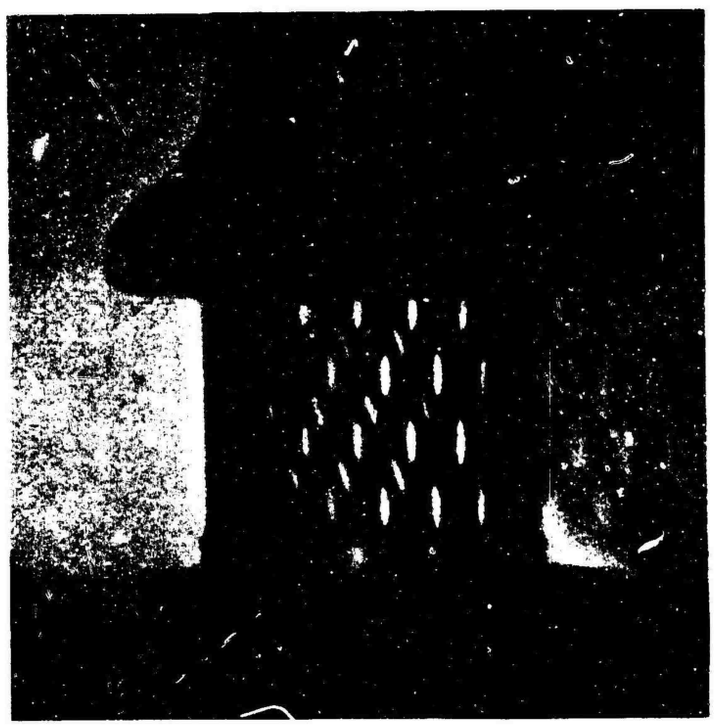

Fig. 26(f)--Final Collapse – Mushroom Mode.

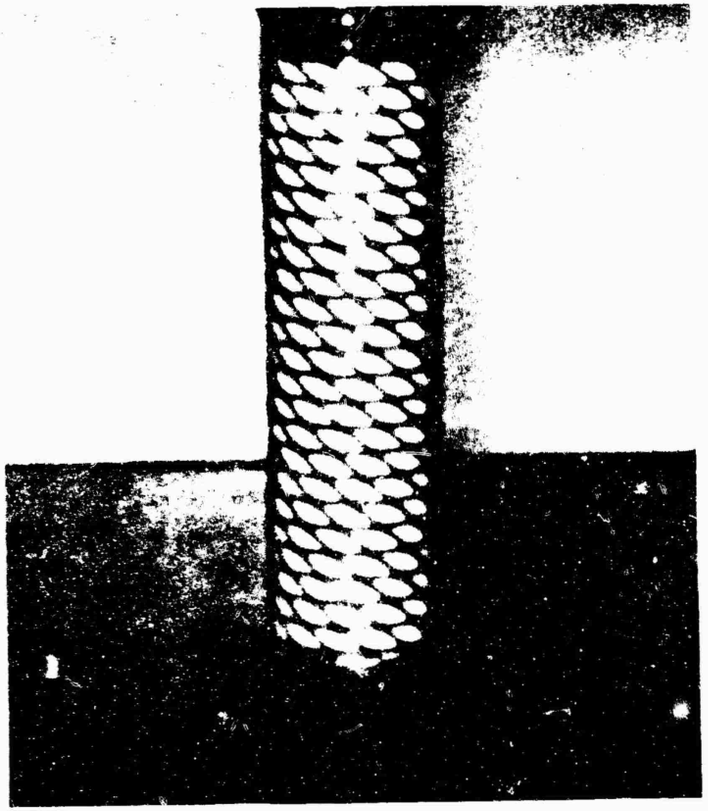

Fig. 26(g)--Long Specimen With Inclined Orientation of Diamond Pattern.

Fig. 26(h)--Collapsed Specimen – Spiral Mode.

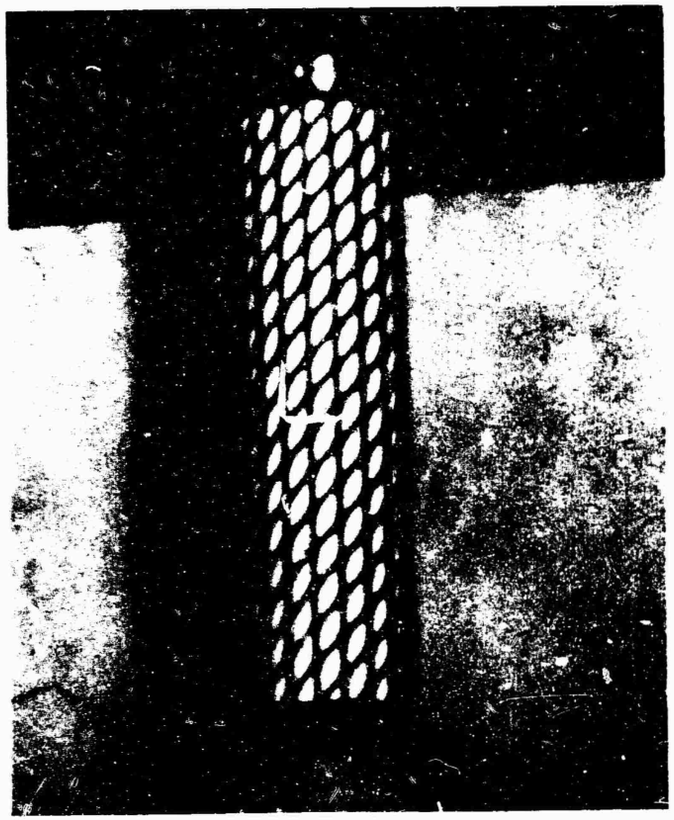

Fig. 26(i)--Long Specimen With Inclined Orientation of Diamond Pattern Loaded by Swivel Joint.

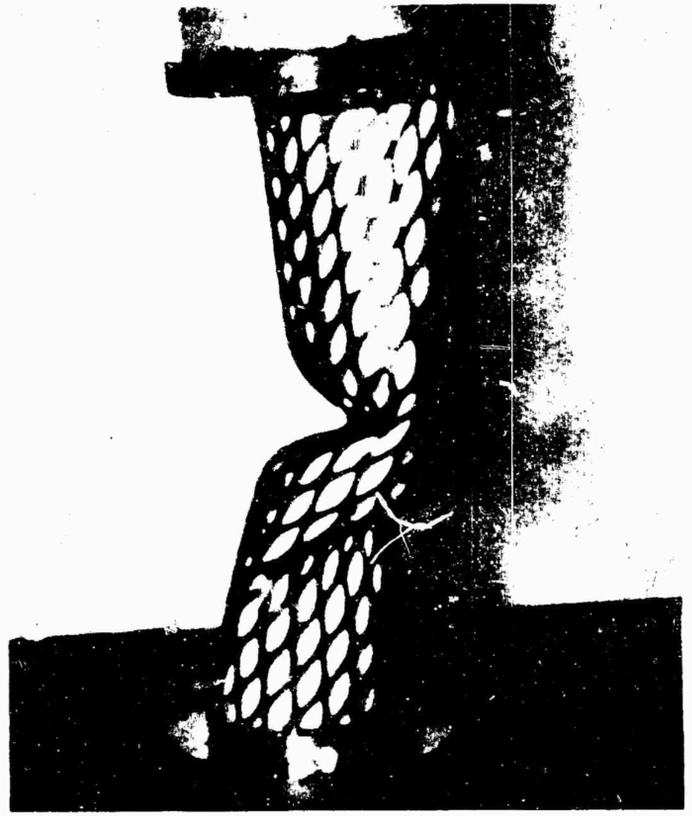

Fig. 26(j)--Collapse Specimen – Euler Torsion Mode.

Fig. 26(k)--Long Specimen With Inclined Orientation of Diamond Pattern – Euler Mode.

References

1. Euler, Methodus inveniendi lineas curvas maximi minimive proprietate gaudentes, sive solutio problematis isoperimetrici latissimo sensu accepti, Additamentum 1, De curvis elasticis, Marcus-Michaelus Bousquet, p. 267, Lausanne and Geneva, 1744.
2. Considère, Résistance des pièces comprimées, Congrès International des Procédés de Construction, Annexe, Librairie Polytechnique, p. 371, Paris, 1891.
3. Engesser, Über Knickfestigkeit gerader Stabe, Zeitschrift des Architekten und Ingenieurvereins zu Hanover, Vol. 35, No. 4, p. 455, 1889.
4. Engesser, Über Knickfragen, Schweizerische Bauzeitung, Vol. 26, No. 4, p. 24, July 27, 1895.
5. Jasinski, Noch ein Wort zu den "Knickfragen," Schweizerische Bauzeitung, Vol. 25, No. 25, p. 172, June 22, 1895.
6. Karman, Untersuchungen über Forschungsarbeiten auf dem Gebiete des Ingenieurwesens, No. 81, Verein Deutscher Ingenieure, Berlin, 1910; see also Collected Works of Theodore von Karman, Vol. 1, p. 90; Butterworths Scientific Publications, London, 1956.
7. Southwell, On the Analysis of Experimental Observations in Problems of Elastic Stability, Proceedings of the Royal Society (A), Vol. CXXXV, 1932, p. 601.
8. Parr and Beakley, An Investigation of Duralumin Channel Section Struts in Compression, Journal of the Aeronautical Sciences, Vol. 3, September 1935, p. 21.
9. Lundquist, Local Instability of Symmetrical Rectangular Tubes Under Axial Compression, NACA Tech. Note 686.
10. Lundquist, Local Instability of Centrally Loaded Columns of Channel Section and Z Section, NACA Tech. Note 722.
11. Hu and McCulloch, The Local Buckling Strength of Lipped Z-Columns With Small Lip Width, NACA Tech. Note 1335, June 1947.
12. Goodman, Elastic Buckling of Outstanding Flanges Clamped at One Edge and Reinforced by Bulbs at Other Edge, NACA Tech. Note 1985, October, 1949.

13. Goodman and Boyd, Instability of Outstanding Flanges Simply Supported at One Edge and Reinforced by Bulbs at Other Edge, NACA Tech. Note 1433, December 1947.

14. Kroll, Fisher, Gordon and Heimeil, Charts for Calculation of the Critical Stress for Local Instability of Columns With I, Z Channel and Rectangular Tube Section, NACA , ARR 3K04, November 1943.

15. Heimeil and Roy, The Determination of Effective Column Length from Strain Measurements , NACA, ARR L4F24, June 1944.

16. Wagner and Pretschner, Torsion and Buckling of Open Sections, NACA Tech Memo 784.

17. Wagner, Torsion and Buckling of Open Sections, NACA Tech Memo 807.

18. Kappus, Twisting Failure of Centrally Loaded Open-Section Columns in the Elastic Range, NACA Tech Memo 851.

19. Lundquist and Fligg, A Theory for Primary Failure of Straight Centrally Loaded Columns, NACA Tech Rep 582.

20. Brigham and Baab, Charts of the Critical Compressive Stress for Local Instability of Idealized Web and T-Stiffened Panels, NACA, ARR L4H.29, August 1944.

21. Lundquist, Stowell and Schuette, Principles of Moment Distribution Applied to Stability of Structures Composed of Bars or Plates, NACA, ARR 3K06, 1943.

22. Goodier, Torsional and Flexual Buckling of Bars of Thin-Walled Open Section Under Compressive and Bending Loads. Journal of Applied Mechanics, Vol. IX, No. 3, September 1942, p. A.103.

23. Hoff, General Instability of Monocoque Cylinders, Journal of the Aeronautical Sciences, Vol. X, No. 4, April 1943, p. 105.

24. Hoff, Instability of Monocoque Structures in Pure Bending, Journal of the Royal Aeronautical Society, Vol. XLII, No. 328, April 1938, p. 291.

25. Hoff, Stresses in a Reinforced Monocoque Cylinder Under Concentrated Symmetrical Transverse Loads, Journal of Applied Mechanics, Vol. XI, No. 4, December 1944, p. A-235.

26. Hoff, Thin-Walled Monocoques, Aeronautical Conference, London, September 1947. Published by the Royal Aeronautical Society, 1948, p. 312.

27. Dow and Hickman, Effect of Variation in Diameter and Pitch of Rivets on Compressive Strength of Panels With Z-Section Stiffeners. Panels That Fail by Local Buckling and Have Various Values of Width-to-Thickness Ratio for the Webs of the Stiffeners, NACA, T.N. 1737, November 1948.

28. Dow and Hickman, Effect of Variation in Diameter and Pitch of Rivets on Compressive Strength of Panels With Z-Section Stiffeners. Panels of Various Lengths With Close Stiffener Spacing, NACA T.N. 1421, September 1947. Panels of Various Stiffener Spacings That Fail by Local Buckling, NACA, T.N. 1467, October 1947.

29. Dow and Hickman, Effect of Variation in Rivet Diameter and Pitch on the Average Stress at Maximum Load for 24 S-T3 and 75 S-T6 Aluminum-Alloy, Flat, Z-Stiffened Panels That Fail by Local Instability, NACA, T.N. 2139, January 1950.

30. Kuhn, The Strength and Stiffness of Shear Webs With and Without Lightening Holes, NACA, ARR L402, June 1942.

31. Kuhn, The Strength and Stiffness of Shear Webs With Round Lightening Holes Having 45° Flanges, NACA, ARR L323, December 1942.

32. Kuhn and Griffith, Diagonal Tension in Curved Webs, NACA T.N. 1481, November 1947.

33. Kuhn and Peterson, Strength Analysis of Stiffened Beam Webs, NACA T.N. 1364, July 1947.

34. Leggett, The Buckling of a Square Panel Under Shear When One Pair of Opposite Edges is Clamped, and the Other Pair is Simply Supported, A.R.C., R. and M. 1991, 1941.

35. Leggett, The Buckling of a Long Curved Panel Under Axial Compression, A.R.C., R. and M. 1899, 1942.

36. Leggett, The Elastic Stability of a Long and Slightly Bent Rectangular Plate Under Uniform Shear, Proc. Roy. Soc., (London), Ser.A, Vol. CLXII, No. 908, September 1937, p. 62.

37. Leggett, The Initial Buckling of Slightly Curved Panels Under Combined Shear and Compression, A.R.C., R. and M. 1972, 1941.

38. Fairbairn, On the Resistance of Tubes to Collapse, Philosophical Transactions of the Royal Society, London, Vol. 148, p. 389, 1859.

39. Bryan, On the Stability of Elastic Systems, Proceedings Cambridge, Philosophical Society, Vol. 6, p. 199, 1888.

40. Lorenz, Achsensymmetrische Verzerrungen in dünnwandigen Hohlzylinder, Zeitschrift des Vereins Deutscher Ingenieure, Vol. 52, No. 43, p. 1706, October 1908.

41. Timoshenko, Einige Stabilitätsprobleme der Ekstizitätstheorie, Zeitschrift für Mathematik un Physik, Vol. 58, No. 4, p. 337, June 1910.

42. Southwell, On the General Theory of Elastic Stability, Philosophical Transactions of the Royal Society, London, Series A, Vol. 213, No. A501, p. 187, August 1913.

43. Robertson, The Strength of Tubular Struts, Proc. Royal Soc., London, Series A, Vol. 121, 1928.

44. Weingarten, Morgan and Seide, Final Report on Development of Design Criteria for Elastic Stability of Thin Shell Structures, Report No. STL/TR-60-0000-19425, Space Technologies Laboratories, Inc., December 1960.

45. Donnell, A New Theory for the Buckling of Thin Cylinders Under Axial Compression and Bending, Transactions of the American Society of Mechanical Engineers, Report AER-56-12, Vol. 56, p. 795, 1934.

46. von Kármán and Tsien, The Buckling of Thin Cylindrical Shells Under Axial Compression, Journal of the Aeronautical Sciences, Vol. 8, No. 8, p. 302, 1941.

47. Yoshimura, On the Mechanism of Buckling of a Circular Cylindrical Shell Under Axial Compression, National Advisory Committee for Aeronautics, Technical Memorandum 1390, Washington, D. C., July 1955.

48. Hoff and Rehfield, Buckling of Axially Compressed Circular Cylindrical Shells at Stresses Smaller Than the Classical Critical Value, SUDAER No. 191, Stanford University, May 1961.

49. Nachbar and Hoff, On Edge Buckling of Axially Compressed Circular Cylindrical Shells, Quarterly of Applied Mathematics, Vol. xx, No. 3, p. 267, October 1962.

50. Stein, The Effect on the Buckling of Perfect Cylinders of Prebuckling Deformations and Stresses, Collected Papers on Instability of Shell Structures, National Aeronautics and Space Administration, Technical Note D-1510, p. 217, 1962.

51. Fischer, "Über den Einfluss der gelenkizen Lagerung auf die Stabilität dünn wandiger Kreiszylinderschalen unter Axiallast und Innerdruck", Zenschrift Flugwissenschaften, Tahrg. 11, Heft 3, p. 111-119, March 1963.

52. Babcock and Sechler, The Effect of End Slope on the Buckling Stress of Cylindrical Shells, NASA TN D-2537, December 1964.

53. Mayers and Rehfield, Further Nonlinear Considerations in the Post-buckling of Axially Compressed Circular Cylindrical Shells, SUDAER No. 197, Stanford University, June 1964.

54. Hoff, Mayers and Madsen, The Postbuckling Equilibrium of Axially Compressed Circular Cylindrical Shells, SUDAER No. 221, Stanford University, February 1965.

55. Lundquist, A New Theory for the Buckling of Thin Cylinders Under Axial Compression and Bending, Trans. ASME, Vol. 56, pp. 795-806, 1934.

56. Flügge, Die Stabilität der Kreiszylinderschale, Ing.-Archiv, Vol. 3, No. 5, December 1932, pp. 463-506.

57. Timoshenko, Theory of Elastic Stability, McGraw-Hill Book Company, Inc., New York, N. Y., 1936, pp. 463-467.

58. Suer, Harris, Skene and Benjamin, The Bending Stability of Thin-Walled Unstiffened Circular Cylinders Including the Effects of Internal Pressure, Jnl. of the Aeronautical Sciences, Vol. 25, No. 5, May 1958, pp. 281-287.

59. Peterson, Bending Tests of Ring-Stiffened Circular Cylinders, NACA TN 3735, July 1956.

60. Harris, Suer, Skene and Benjamin, The Stability of Thin-Walled Unstiffened Circular Cylinders Under Axial Compression Including the Effects of Internal Pressure, Jnl. of the Aeronautical Sciences, Vol. 24, No. 8, August 1957, pp. 587-596.

61. Bijlaard and Gallagher, Elastic Instability of a Cylindrical Shell Under Arbitrary Circumferential Variation of Axial Stress, Jnl. of the Aero/Space Sciences, Vol. 27, No. 11, 1960, pp. 854-858, 866.

62. Seide and Weingarten, On the Buckling of Circular Cylindrical Shells Under Pure Bending, Jnl. of Applied Mechanics, ASME, March 1961, pp. 112-116.

63. Abir and Nardo, Thermal Buckling of Circular Cylindrical Shells Under Circumferential Temperature Gradients, Jnl. of the Aero/Space Sciences, Vol. 26, No. 12, pp. 803-808, December 1959.

64. Holmes, Compression Tests on Thin-Walled Cylinders, Aeronautical Quarterly, Vol. 12, May 1961.

65. Babcock and Sechler, The Effect of Initial Imperfections on the Buckling Stress of Cylindrical Shells, Collected Papers on Instability of Shell Structures, National Aeronautics and Space Administration, Technical Note D-1510, p. 135, 1962.

66. Almroth, Holmes and Brush, An Experimental Study of the Buckling of Cylinders Under Axial Compression, Experimental Mechanics, p. 263-270, September 1964.

67. Tennyson, An Experimental Investigation of the Buckling of Circular Cylindrical Shells in Axial Compression Using the Photoelastic Technique, UTIAS Report No. 102, University of Toronto, November 1964.

68. Horton and Durham, Repeated Buckling of Circular Cylindrical Shells and Conical Frusta by Axial Compressive Forces, SUDAER No. 175, Stanford University, November 1963.

69. Horton and Durham, The Effect of Restricting Buckle Depth in Circular Cylindrical Shells Repeatedly Compressed to the Buckling Limit, SUDAER No. 174, Stanford University, September 1963.

70. Horton and Durham, Imperfections, A Main Contributor to Scatter in Experimental Values of Buckling Load, To be published in the International Journal of Solids and Structures, 1965.

71. Horton and Cox, The Stability of Thin-Walled Unstiffened Circular Cylindrical Shells Under Nonuniformly Distributed Axial Load, SUDAER No. 220, Stanford University, February 1965.

72. Tsien, A Theory of the Buckling of Thin Shells, Journal of the Aeronautical Sciences, Vol. 9. No. 10, p. 373, August 1942.

73. Horton and Bailey, The Significance of Test Machine Rigidity on the Initial Buckling Load for Unreinforced Circular Cylindrical Shells in Axial Compression. (To be presented at ASTM Annual Meeting, June 1966).

74. Bijlaard, On the Plastic Stability of Thin Plates and Shells, Prov. Kon. Akad. v. Wetensch., Amsterdam, p. 765, 1949.

75. Bijlaard, Theory and Tests on the Plastic Stability of Plates and Shells, Journal of the Aeronautic Sciences, Vol. 16, p. 529, September 1949.

76. Gerard, Compressive and Torsional Buckling of Thin-Walled Cylinders in Yield Region, National Advisory Committee for Aeronautics, Technical Note 3726, August 1956.

77. Geckeler, Plastisches Knicken der Wandun von Hohlzylindern und einige andere Faltunserscheinungen an Schalen und Blechen, Zeitschrift für Angewandte Mathematik und Mechanik, Band 8, Heft 5, p. 23, October 1928.

78. Batterman, Plastic Buckling, AIAA Journal, Vol. 3, No. 2, p. 316, February 1965.

79. Mayers, Nelson and Smith, The Maximum Strength of Rectangular Postbuckled Plates in Compression, SUDAER No. 215, Stanford University, December 1964.